THE ASTROPHYSICAL JOURNAL, 477:128–143, 1997 March 1

THE IRON DISCREPANCY IN ELLIPTICAL GALAXIES AFTER *ASCA*

NOBUO ARIMOTO
Institute of Astronomy, University of Tokyo, Mitaka, Tokyo 181, Japan
KYOKO MATSUSHITA AND YUHRI ISHIMARU
Department of Astronomy, University of Tokyo, Bunkyo-ku, Tokyo 113, Japan
TAKAYA OHASHI
Department of Physics, Tokyo Metropolitan University, Hachioji, Tokyo 192-03, Japan
AND
ALVIO RENZINI[1]
European Southern Observatory, Karl-Schwarzschild-Strasse 2, D-85748, Garching bei München, Germany
Received 1996 May 6; accepted 1996 September 3

ABSTRACT

We present estimates for the iron content of the stellar and diffused components of elliptical galaxies, as derived respectively from integrated optical spectra and from *ASCA* X-ray observations. A macroscopic discrepancy emerges between the expected iron abundances in the hot interstellar medium (ISM) and what is indicated by the X-ray observations, especially when allowance is made for the current iron enrichment by Type Ia supernovae. This strong discrepancy, that in some extreme instances may be as large as a factor of ~ 20, calls into question our current understanding of supernova enrichment and chemical evolution of galaxies. We discuss several astrophysical implications of the inferred low iron abundances in the ISM, including the chemical evolution of galaxies and clusters of galaxies, the evolution of gas flows in elliptical galaxies, and the heating of the intracluster medium. Some of the consequences appear hard to accept, and in the attempt to avoid some of the difficulties we explore ways of hiding or diluting iron in the ISM of ellipticals. None of these possibilities appears astrophysically plausible, and we alternatively raise the question of the reliability of iron L line diagnostic tools that are currently used to infer abundances from X-ray spectra. Various thin-plasma emission models are shown to give iron abundances that may differ significantly, especially at low temperatures ($kT \lesssim 1$ keV), when the iron L complex is dominated by iron ions with still many bound electrons. From a collection of *ASCA* and other X-ray observatory data, it is shown that current thin-plasma codes tend to give very low iron abundances when the temperature of the objects is below ~ 1 keV. Such objects include various types of binary stars, supernova remnants, starburst galaxies, and AGNs, with the case of galaxy groups being especially well documented. We conclude that, besides rethinking the chemical evolution of galaxies, one should also consider the possibility that existing thin-plasma models may incorporate inaccurate atomic physics for the ions responsible for the iron L complex.

Subject headings: atomic processes — galaxies: abundances — galaxies: elliptical and lenticular, cD — galaxies: ISM — X-rays: galaxies

1. INTRODUCTION

Stars in elliptical galaxies lose about one-third of their mass while ascending the red giant branches and before dying as white dwarfs. The interstellar medium (ISM) of these galaxies is therefore continuously replenished with gas, which is soon heated to X-ray temperatures by the collision of the red giant winds with the ISM, by supernova (SN) explosions, and—in the case of inflows—by the $P\,dV$ work due to gravitational compression. Hence the chemical composition of the ISM is expected to reflect the average composition of the stellar component as established at the time of its formation and then further enriched by SNs of Type Ia that currently explode in elliptical galaxies. This additional enrichment is expected to be especially important for iron, as this is the main nucleosynthetic contribution of SN Ia's (Nomoto, Thielemann, & Yokoi 1984). On these premises, the iron abundance in the hot ISM is expected to be

$$Z_{\rm ISM}^{\rm Fe} = \langle Z_*^{\rm Fe} \rangle + 5\vartheta_{\rm SN}\left(\frac{M^{\rm Fe}}{0.7\ M_\odot}\right)h_{50}^2 \qquad (1)$$

(Ciotti et al. 1991; Renzini et al. 1993, hereafter RCDP), where $\langle Z_*^{\rm Fe} \rangle$ is the average iron abundance of the stars in units of the solar abundance, $h_{50} \equiv H_0/50$ is the Hubble constant in units of 50 km s^{-1} Mpc^{-1}, and $\vartheta_{\rm SN}$ is the present rate of SN Ia's in ellipticals in units of the rate as estimated by Tammann (1982), or 2.2×10^{-13} SNs $L_\odot^{-1}$ yr^{-1}. Current estimates of the iron yield ($M^{\rm Fe}$) per SN Ia event cluster around 0.7 $M_\odot$ of iron (Nomoto et al. 1984; Shigeyama et al. 1992; Woosley & Weaver 1994; Nomoto et al. 1996).

Note that increasing the Hubble constant has the effect of increasing the expected iron enrichment from SN Ia's. This occurs because the SN rate per unit galaxy luminosity increases as the luminosity decreases with a shorter distance scale, while the actual number of observed SN events clearly stays the same. However, part of this effect may be compen-

[1] On leave from Dipartimento di Astronomia, Università di Bologna.

sated by the estimated iron yield per SN Ia event being itself dependent on the distance scale, as it is based on fitting the SN light curve. Still, this compensation cannot be complete, since at least 0.4 $M_\odot$ needs to be incinerated to nuclear statistical equilibrium (and eventually processed to iron) in order to unbound the star and impart to the SN photosphere the observed high velocity (Arnett, Branch, & Wheeler 1985). When bearing in mind that the 0.7 $M_\odot$ estimate of Nomoto et al. (1984) is based on the assumption $h_{50} = 1$, we can guess $M^{\rm Fe} = 0.4\ M_\odot$ to be more appropriate for the choice $h_{50} = 2$. This still implies a more pronounced iron enrichment by SN Ia's if a short distance scale is assumed.

From optical observations the stellar iron abundances in early-type galaxies are believed to range from $\sim\frac{1}{3}$ solar for dwarf ellipticals such as M32 (Freedman 1989) to a few times solar for giant ellipticals (e.g., O'Connell 1986; Bica 1988). The iron enrichment due to SN Ia's is critically sensitive to the adopted SN rate in ellipticals, a quantity that is still affected by a major uncertainty. A high value ($\vartheta_{\rm SN} = 1.1$) virtually identical to the old estimate of Tammann (1982) was reported by van den Bergh & Tammann (1991). On the other hand, Cappellaro et al. (1993) estimate a substantially lower value ($\vartheta_{\rm SN} = 0.25$). Thus, combining into equation (1) the estimated stellar abundances with the SN contribution, we estimate the expected iron abundance in the hot ISM of elliptical galaxies to range from a minimum of ~ 2 times solar to perhaps as much as ~ 5 times solar or more, depending on the adopted SN Ia rate.

The determination of the iron abundance of the hot ISM of elliptical galaxies offers the opportunity to check at once the average stellar metallicity as estimated from optical observations, and the expected contribution from SN Ia's. The latter aspect is particularly important because this SN rate is one of the key parameters controlling the gas flow regime that is established in hydrodynamical models of elliptical galaxies (Ciotti et al. 1991; Renzini 1994a). As extensively discussed by these authors, crucial for the evolution of the gas flows over cosmological times is also the secular evolution of the SN Ia heating after the completion of the bulk of star formation in these galaxies. For exploratory purposes such heating can be assumed to decline with time as a power law, i.e., $\propto t^{-s}$, a convenient parameterization. In the absence of other energy sources, the gas flows evolve from early supersonic winds to subsonic outflows, and eventually to inflows if $s \gtrsim 1.3$. Conversely, the reverse sequence of flow regimes is established if $s \lesssim 1.3$, with early inflows turning to outflows and winds at later times (Loewenstein & Matthews 1991; David, Forman, & Jones 1990). The epoch of transition from one flow regime to another is very sensitive to several galaxy parameters, especially to its mass, luminosity, structure, and SN rate. Since both SN heating and iron enrichment of the ISM depend on the assumed SN rate, it was soon realized that the determination of the iron abundance in the ISM could lead to a welcome reduction in the number of parameters, thus setting an important constraint on the evolution of gas flows in galaxies.

An estimate of the iron abundance in elliptical galaxy flows was first attempted using data from the *Ginga* satellite. Ohashi et al. (1990) reported an upper limit about twice solar for NGC 4472 and NGC 4636. From the upper limit to the iron line equivalent width reported by Awaki et al. (1991) for NGC 4472, Ohashi & Tsuru (1992) estimate the iron abundance in the flow to be at most solar. For NGC 1399—the cD galaxy in the Fornax Cluster—Ikebe et al. (1992) estimate iron to be $1.1^{+1.3}_{-0.5}$ times solar. From BBXRT observations and one-temperature fits Serlemitsos et al. (1993) estimate the metallicity of NGC 1399 and NGC 4472 to be at 90% confidence $0.56^{+0.82}_{-0.38}$ and $0.20^{+0.46}_{-0.09}$, respectively, while from *ROSAT* observations Forman et al. (1993) infer iron to be 1–2 times solar in NGC 4472.

Iron abundance determinations in elliptical galaxy flows has then gained great impetus by the advent of the *ASCA* satellite, thanks to its superior spectral energy resolution. The low iron abundances appear to be confirmed by *ASCA* observations (Awaki et al. 1994; see also § 2.2) that indicate, e.g., for NGC 4472 an iron abundance $0.52^{+0.09}_{-0.07}$ at the 90% confidence level.

There is clearly a macroscopic discrepancy between the expected abundance, even with the lowest SN Ia enrichment, and what is consistently indicated by the X-ray observations of elliptical galaxies with four different X-ray telescopes: BBXRT and those on board *Ginga*, *ROSAT*, and *ASCA*. Instrumental problems, such as calibrations and the like, can therefore be firmly excluded as the origin of this *iron discrepancy*. Note also that the discrepancy is exacerbated by another factor of ~ 2 if a short distance scale is adopted ($h_{50} = 2$). We believe that the solution of the discrepancy, whatever it is, will have profound implications for our understanding of galaxy formation and evolution and/or for the X-ray diagnostics of astronomical objects, and in this paper we thoroughly address the question. In § 2 we present and discuss the state of the art estimates for the iron content of the stellar and diffused components of elliptical galaxies, as derived respectively from integrated optical spectra and X-ray observations. In § 3 we discuss several astrophysical implications of the observed low iron abundances in the ISM, assuming these determinations to give the actual abundance to be compared with the prediction of equation (1). These implications include the role of SN Ia's in ellipticals, the chemical evolution of these galaxies, as well as the enrichment and heating of the intracluster medium. Having encountered several astrophysical difficulties that are generated by this assumption, in § 4 we explore various alternative possibilities of hiding or diluting iron in the ISM, so as to reconcile the expectations with the X-ray observations. These possibilities include dilution of the ISM with iron-poor gas from an intracluster medium (ICM), as well as astration from the ISM, in the form of either particulates (iron flakes) or substellar mass objects (jupiters). None of the explored solutions appears very attractive or astrophysically plausible, and in § 5 we alternatively raise the question of the reliability of iron line diagnostic tools that are currently used in conjunction with X-ray observations. At the temperatures that are typical of the hot ISM of elliptical galaxies ($\lesssim 1$ keV), the iron abundance is derived from the strength of several lines originated by electron transitions down to the L shell in incompletely ionized iron ions, typically Fe XVIII–Fe XXI, hence called "iron L." Conversely, X-ray iron K lines are due to electron decays to the K shell of He-like and H-like iron ions. In § 5 we compare the results of iron L diagnostics at different temperatures according to different thin-plasma models, and finally we list and discuss the iron abundance in a variety of astrophysical objects as derived from *ASCA* data and current iron L diagnostics. Our conclusions are presented in § 6.

2. IRON CONTENT OF ELLIPTICAL GALAXIES

2.1. *Iron Abundance in the Stellar Component*

As already mentioned, the stellar iron abundances in early-type galaxies are believed to range from $\sim\frac{1}{3}$ solar in dwarf ellipticals such as M32 to a few times solar in giant elliptical galaxies. From a theoretical work, which itself is an extended version of Larson's (1974) supernova-driven galactic wind model, Arimoto & Yoshii (1987) first obtained a stellar metallicity distribution ranging from $\sim 1/10$ solar to about 10 times solar for the bulk of stars in a giant elliptical galaxy, with a luminosity-weighted mean ~ 2 times solar. Such a huge amount of heavy elements is produced during an intensive phase of star formation in the early stage of galaxy formation. Because the broadband colors of ellipticals are well matched by Arimoto & Yoshii (1987) models, it has been widely accepted that giant elliptical galaxies are super–metal-rich, at least ~ 2 times solar or even more.

In this section the iron abundance is derived from the observed Mg_2 indices by using the relation given by the population synthesis model of Buzzoni, Gariboldi, & Mantegazza (1992):

$$[\mathrm{Fe/H}] = 7.41\mathrm{Mg}_2 - 2.07 \, . \tag{2}$$

The population synthesis models of Worthey (1994) give a slightly different calibration, i.e., $[\mathrm{Fe/H}] = 5.85\mathrm{Mg}_2 - 1.66$, but the resulting values of [Fe/H] are almost identical to those calculated with equation (2). We note that both relations give considerably steeper slopes than the early population synthesis models by Mould (1978), for which $[\mathrm{Fe/H}] = 3.9\mathrm{Mg}_2 - 0.9$.

Giant elliptical galaxies usually exhibit conspicuous color and metallic line-strength gradients (e.g., Franx, Illingworth, & Heckman 1989; Peletier et al. 1990; Gorgas, Efstathiou, & Aragón-Salamanca 1990; Davies, Sadler, & Peletier 1993). This implies a negative radial gradient of the stellar metallicity, and therefore the true *mean* iron content of an elliptical galaxy may be appreciably lower than the value indicated by colors or spectral features taken at the galaxy center.

The line-strength gradients in elliptical galaxies are considered to provide clues to the importance of dissipative processes in galaxy formation (Larson 1976; Carlberg 1985). In an early study, Faber (1977) first measured the radial gradient in the Mg_2 index for NGC 4472 and reported that the contour of constant line strength tends to be flatter than the isophote, in agreement with Larson's dissipative collapse models. In recent years, the line-strength gradients have attracted much attention (e.g., Efstathiou & Gorgas 1985; Baum, Thomsen, & Morgan 1986; Thomsen & Baum 1987; Couture & Hardy 1988; Gorgas et al. 1990; Boroson & Thompson 1991; Delisle & Hardy 1992; Davies et al. 1993; Carollo & Danziger 1994a, 1994b) bringing above ~ 40 the number of elliptical galaxies with measured line-strength gradients. In this section, we present a general method to estimate the mean iron abundance of stars in an elliptical galaxy that takes gradients into account, and give the resulting iron contents for ~ 40 galaxies with known line-strength gradients.

It is widely known that the surface brightness distributions of elliptical galaxies are well fitted by the so-called $r^{1/4}$ law (de Vaucouleurs 1948):

$$I(r) = I_e \exp\left\{-b\left[\left(\frac{r}{r_e}\right)^{1/4} - 1\right]\right\}, \tag{3}$$

where $b = 3.33 \ln 10$ and the length scale r_e is the effective radius, interior to which one-half of the total light of the galaxy is emitted. Thus, the total luminosity (e.g., L_B) is given by

$$L_B = \int_0^\infty 2\pi r I(r) dr = 8\pi r_e^2 I_e e^b \Gamma(8) b^{-8} \, , \tag{4}$$

where Γ is the gamma function.

For the radial distributions of the iron abundance $Z^{\mathrm{Fe}}(r)$ we adopt the convenient parameterization

$$Z^{\mathrm{Fe}}(r) = Z^{\mathrm{Fe}}(r_e)\left(\frac{r}{r_e}\right)^{-c} , \tag{5}$$

where both $Z^{\mathrm{Fe}}(r_e)$ and the *slope* parameter c can be derived from the line-strength measurements after properly transforming the line index to the iron abundance. Usually the line-strength measurements do not reach much beyond the effective radius, but here we assume that equation (5) holds for the whole galaxy, a reasonable approximation in most cases. Indeed, only few ellipticals show steeper line-strength or color gradients beyond r_e, such exceptions being, e.g., NGC 5813 (Gorgas et al. 1990), NGC 4697 (Franx et al. 1989), and NGC 4889 (Peletier et al. 1990). The total iron mass locked in the stars is then given by

$$\begin{aligned} M^{\mathrm{Fe}} &= \left(\frac{M_*}{L_B}\right)\int_0^\infty 2\pi Z^{\mathrm{Fe}}(r_e) r I(r)\left(\frac{r}{r_e}\right)^{-c} dr \\ &= 8\pi r_e^2 I_e \left(\frac{M_*}{L_B}\right) Z^{\mathrm{Fe}}(r_e) e^b \Gamma(8-4c) b^{-(8-4c)} \\ &= M_* \frac{\Gamma(8-4c)}{\Gamma(8)} b^{4c} Z^{\mathrm{Fe}}(r_e) \, , \end{aligned} \tag{6}$$

where M_* is the total stellar mass. In deriving equation (6) the stellar mass-to-light ratio is assumed to be constant throughout a galaxy. The mean iron abundance of stars is then given by

$$\begin{aligned} \langle Z_*^{\mathrm{Fe}} \rangle \equiv \frac{M^{\mathrm{Fe}}}{M_*} &= \frac{\Gamma(8-4c)}{\Gamma(8)} b^{4c} Z^{\mathrm{Fe}}(r_e) \\ &= \beta(c) Z^{\mathrm{Fe}}(r_e) \, , \end{aligned} \tag{7}$$

where $\beta(c) \equiv b^{4c}\Gamma(8-4c)/\Gamma(8)$. Equation (7) can also be written as

$$\langle [\mathrm{Fe/H}] \rangle = [\mathrm{Fe/H}]_{r_e} + \log \beta(c) \, , \tag{8}$$

and the function $\beta(c)$ is, with a few exceptions, close to unity for the observed range of c-values, as shown in Figure 1. Thus, *the mean, luminosity-weighted iron abundance of stars in an elliptical galaxy is to a good approximation given by a value measured at the effective radius* r_e, *or* $\langle [\mathrm{Fe/H}] \rangle \simeq [\mathrm{Fe/H}]_{r_e}$. A correction to $[\mathrm{Fe/H}]_{r_e}$ is at most $+0.3$ dex, but usually less than $+0.2$ dex.

Note that the observed Mg_2 gradients coupled with the calibrations by Buzzoni et al. (1992) and Worthey (1994) give an average iron abundance gradient $\Delta[\mathrm{Fe/H}]/\Delta \log r = -0.5 \pm 0.2$, or a reduction by 50%–80% over a factor of 10 in radius—a significant reduction that is consistent with the dissipative models (Larson 1974; Carlberg 1985).

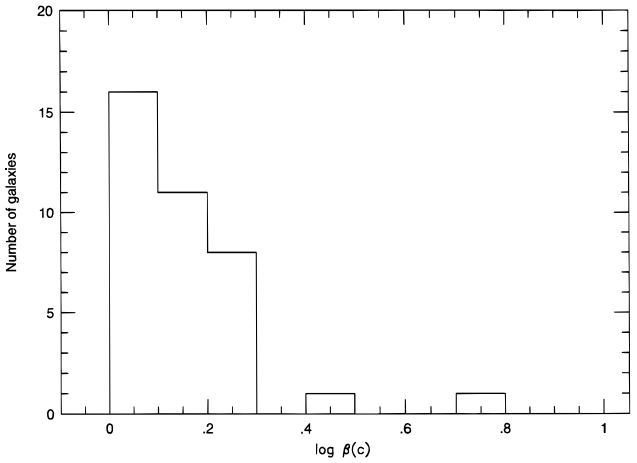

FIG. 1.—Histogram of the correction factor $\beta(c)$ calculated for our sample of elliptical galaxies listed in Table 1. The luminosity-weighted iron abundance of a whole galaxy is given by the product of $\beta(c)$ times the luminosity-weighted abundance as measured at the galaxy effective radius. Two galaxies with $\log \beta(c) > 0.4$ are NGC 1453 and NGC 3962.

Table 1 gives the resulting mean iron abundances of stars in the sample of elliptical galaxies; column (2) gives r_e in arcseconds with the corresponding reference in column (3); columns (4) and (5) give the Mg_2 index at galaxy center and at $r = r_e$, respectively, with the corresponding source in column (7); column (6) gives the Mg_2 gradient defined as $d \equiv \Delta Mg_2/\Delta \log r$. A value of d is estimated for each galaxy by applying a linear least-squares fit to the observed Mg_2 values except for the innermost region with $\log (r/r_e) \lesssim -1.0$. Columns (8) and (9) give central and mean iron abundances, respectively, the latter from equation (8); finally, column (10) gives the stellar velocity dispersion at galaxy center from Davies et al. (1987). The iron abundance *slope* is then given as $c = -7.41\,d$, where we have used equation (2). It appears that in galaxies with $\sigma_0 \gtrsim 250$ km s^{-1} the average *central* iron abundance is in the range $[\mathrm{Fe/H}]_0 \simeq 0.24 \pm 0.10$, while the *mean* iron abundance is $\langle[\mathrm{Fe/H}]\rangle \simeq -0.06 \pm 0.13$, i.e., a factor of ~ 2 lower ($\sim$ solar).

In essence these values are luminosity-averaged abundances, the weighting luminosity being that of the continuum in the vicinity of the Mg_2 feature (i.e., about L_V-averaged). Accordingly, they should be regarded as lower limits to the *mass-averaged* iron abundance, since the most metal-rich components in the distribution of metallicity have lower L_V luminosity for a given mass M_* (Greggio 1997). The size of the effect is very sensitive to the detailed metallicity distribution, and for the closed-box model the mass-averaged abundance can be ~ 2 times larger than the luminosity-averaged abundance. Hence, the values of $\langle[\mathrm{Fe/H}]\rangle$ in Table 1 should be regarded as lower limits.

2.2. *Iron Abundance in the Hot ISM*

With its two detectors (SIS and GIS), the *ASCA* X-ray astronomy satellite is capable of performing, with high energy resolution, imaging and spectroscopic observations simultaneously over the energy range from 0.4 to 10 keV (Tanaka, Inoue, & Holt 1994; Ohashi et al. 1996; Makishima et al. 1996). A number of emission lines from elements such as oxygen, silicon, sulfur, and iron can be identified, and the intensity of these lines allows the determination of the abundances in the hot ISM; iron abundances for several elliptical galaxies have already been reported (Awaki et al. 1994; Loewenstein et al. 1994; Mushotzky et al. 1994).

ASCA has also directly confirmed the presence of a hard X-ray component with $kT > 2$ keV (Matsushita et al. 1994), which was suggested by *Einstein* and *ROSAT* observations of low L_X/L_B elliptical galaxies (Kim, Fabbiano, & Trinchieri 1992; Fabbiano, Kim, & Trinchieri 1994). The luminosity of the hard component of the observed galaxies is similar to the contribution by discrete sources as estimated by Canizares, Fabbiano, & Trinchieri (1987) for spiral galaxies. That is, the number of low-mass X-ray binaries (LMXRBs) per unit blue luminosity that emit the hard component appears to be the same in ellipticals as in spirals. We therefore assume that the hard component due to the discrete sources is harder than 5 keV when fitted with bremsstrahlung spectrum. It is worth noting that the lower limit to the abundance is not so sensitive to the adopted temperature of the hard components for $kT_{\mathrm{hard}} \gtrsim 2$ keV, but the upper limit can instead become quite large.

ASCA data are now available for several elliptical galaxies, and for a subsample of them (NGC 720, NGC 1399, NGC 1404, NGC 4374, NGC 4406, NGC 4472, and NGC 4636) we have reanalyzed the spectra and determined the iron abundances with several different plasma models (see also § 5.1). These are all bright ellipticals, with L_B ranging from $\sim 10^{10}$ to $10^{11}\ L_\odot$, and fairly high L_X/L_B ratio. For low L_X/L_B galaxies the hard component dominates the spectra, and it is difficult to determine the ISM abundance; thus these galaxies are not considered in this paper. The observed galaxies are located in a variety of physical environments; NGC 4406, NGC 4374, NGC 4472, and NGC 4636 are in the Virgo Cluster. *Ginga* detected the dense ICM around these galaxies except for NGC 4636 (Takano 1989). NGC 4636 is far from the Virgo Cluster center and is surrounded by very extended X-ray emission characteristics of the group (Trinchieri et al. 1994). NGC 1399 is the cD galaxy in the Fornax Cluster, and NGC 1404 is located near NGC 1399. *ASCA* detects the ICM of the cluster around these galaxies (Ikebe 1996). Therefore, NGC 720 is the only truly isolated system, and others may be within the ICM.

We have integrated the SIS and the GIS spectral data within a radius of 3′ for low L_X/L_B galaxies [$\log (L_X/L_B) < 30.7$], and within 5′ for high L_X/L_B galaxies. The background was removed by subtracting a spectrum of a blank sky emission of the same area using the same part of the detector. For NGC 720, NGC 1399, NGC 4472, and NGC 4636, the background has been removed by subtracting a spectrum of a blank sky emission of the same area using the same part of the detector. For NGC 1404, NGC 4374, and NGC 4406, there is emission from the surrounding ICM, so that we also subtract the surrounding ICM as background; thus we accumulate spectra over the region of the same radius whose angular distance to the optical axis of the XRT is nearly the same as the background spectra. For NGC 1404, the region accumulated as the background is nearly at the same angular distance to the cD galaxy, NGC 1399. The spectra have then been fitted with both χ^2 and maximum likelihood methods using XSPEC spectral fitting package (Raymond & Smith 1977). Both methods give nearly identical results, so we discuss only the results with

TABLE 1

MEAN STELLAR IRON ABUNDANCES OF ELLIPTICAL GALAXIES

Galaxy (1)	r_e (2)	Reference (3)	$Mg_2(0)$ (4)	$Mg_2(r_e)$ (5)	d (6)	Reference (7)	$[Fe/H]_0$ (8)	$\langle[Fe/H]\rangle$ (9)	σ_0 (10)
NGC 315	32	1	0.283	0.282	−0.031	1	0.03	0.05	352
NGC 439	45	2	...	0.231	−0.053	2	...	−0.27	...
NGC 741	50	3	0.324	0.234	−0.057	7	0.34	−0.23	280
NGC 741	42	1	0.324	0.240	−0.058	1	0.34	−0.18	280
NGC 1052.....	30	4	0.316	0.261	−0.061	4	0.28	−0.02	206
NGC 1453.....	30	3	0.327	0.168	−0.118	7	0.36	−0.37	290
NGC 1600.....	34	1	0.324	0.257	−0.088	1	0.34	0.08	321
NGC 2434.....	24	2	0.268	0.187	−0.040	2	...	−0.63	205
NGC 2663.....	50	5	0.324	0.269	−0.051	5	...	0.01	281
NGC 2693.....	17	3	0.328	0.273	−0.041	7	0.37	0.01	279
NGC 3379.....	45	3	0.308	0.204	−0.073	7	0.22	−0.39	201
NGC 3379.....	56	1	0.308	0.238	−0.065	1	0.22	−0.17	201
NGC 3379.....	56	4	0.308	0.261	−0.064	4	0.22	0.00	201
NGC 3665.....	34	1	0.296	0.254	−0.022	1	0.12	−0.17	205
NGC 3706.....	27	2	0.310	0.216	−0.062	2	...	−0.35	...
NGC 3818.....	19	6	0.315	0.236	−0.083	6	0.27	−0.10	206
NGC 3904.....	19	6	0.312	0.228	−0.084	6	0.24	−0.15	215
NGC 3962.....	33	3	0.306	0.129	−0.146	7	0.20	−0.38	211
NGC 4261.....	41	1	0.330	0.271	−0.068	1	0.38	0.09	294
NGC 4278.....	39	3	0.291	0.223	−0.066	7	0.09	−0.28	266
NGC 4278.....	30	1	0.291	0.234	−0.088	1	0.09	−0.09	266
NGC 4283.....	9	3	0.268	0.233	−0.052	7	−0.08	−0.26	100
NGC 4365.....	53	4	0.300	0.263	−0.066	4	0.15	0.02	248
NGC 4374.....	53	1	0.305	0.262	−0.050	1	0.19	−0.05	287
NGC 4406.....	70	4	0.311	0.257	−0.031	4	0.23	−0.13	250
NGC 4472.....	99	1	0.306	0.297	−0.028	1	0.20	0.16	287
NGC 4472.....	99	6	0.306	0.275	−0.042	6	0.20	0.03	287
NGC 4478.....	15	6	0.253	0.229	−0.014	6	−0.20	−0.36	149
NGC 4486.....	76	3	0.289	0.177	−0.125	7	0.07	−0.24	361
NGC 4486.....	95	1	0.289	0.270	−0.076	1	0.07	0.12	361
NGC 4621.....	42	4	0.328	0.265	−0.034	4	0.37	−0.07	240
NGC 4636.....	67	1	0.311	0.236	−0.077	1	0.23	−0.13	191
NGC 4742.....	23	6	0.177	0.175	−0.030	6	−0.76	−0.74	93
NGC 4839.....	42	1	0.315	0.246	−0.058	1	0.26	−0.14	259
NGC 4874.....	67	3	0.328	0.219	−0.060	8	0.37	−0.33	245
NGC 4881.....	11	3	0.293	0.225	−0.088	9	0.10	−0.15	219
NGC 4915.....	9	3	0.291	0.230	−0.044	7	0.09	−0.30	209
NGC 5018.....	22	5	0.209	0.209	−0.034	5	...	−0.48	223
NGC 5638.....	24	6	0.317	0.262	−0.040	6	0.28	−0.07	159
NGC 5813.....	44	6	0.308	0.157	−0.120	10	0.21	−0.43	238
NGC 5813.....	44	6	0.308	0.175	−0.089	6	0.21	−0.52	238
NGC 5831.....	27	6	0.289	0.206	−0.060	6	0.07	−0.43	166
NGC 5845.....	8	6	0.304	0.270	−0.049	6	0.18	0.01	251
NGC 6407.....	33	2	...	0.255	−0.035	2	...	−0.14	...
NGC 7192.....	28	2	0.250	0.188	−0.084	2	...	−0.45	185
NGC 7332.....	17	4	0.278	0.243	−0.061	4	−0.01	−0.15	...
NGC 7626.....	34	1	0.336	0.262	−0.063	1	0.42	0.00	234
IC 4296	48	6	0.323	0.200	−0.087	6	0.32	−0.35	323
2354−35	80	6	0.285	0.248	−0.021	6	0.04	−0.22	316

REFERENCES TO COLUMNS (3) AND (7).—(1) Davies et al. 1993; (2) Carollo & Danziger 1994b; (3) Kodaira et al. 1990; (4) Couture & Hardy 1988; (5) Carollo & Danziger 1994a; (6) Gorgas et al. 1990; (7) Davidge 1992; (8) Baum et al. 1986; (9) Thomsen & Baum 1987; (10) Efstathiou & Gorgas 1985.

the χ^2 method. Thin thermal plasma models modified by interstellar absorption with solar abundance ratios are fitted to each galaxy, and a bremsstrahlung spectrum is assumed for the hard component. The iron abundances are determined from the iron L blends around 1 keV, and the fitting results of 90% confidence are given in Table 2, assuming the solar iron abundance to be 4.68×10^{-5} by number. The derived temperatures of the ISM are in the range from $\sim$0.6 to $\sim$1.1 keV, while the iron abundance range from $\sim$0.1 solar to $\sim$0.4 solar. XSPEC further returns hydrogen column densities of $\sim 10^{21}$ cm^{-2}, significantly higher than Galactic values [$\sim(1\text{–}3) \times 10^{20}$ cm^{-2}]. The temperature and the iron abundances obtained here are consistent with the results by *Ginga* and BBXRT observations (Awaki et al. 1991; Ikebe et al. 1992; Serlemitos et al. 1993). We note that the fit parameters are consistent with *ROSAT* results for NGC 4636 (Trinchieri et al. 1994), but we disagree with the *ROSAT* observation for NGC 4472 (Forman et al. 1993). The iron abundance obtained by *ROSAT* for NGC 4472 is consistent with being

TABLE 2

IRON IN THE HOT ISM OF ELLIPTICAL GALAXIES FROM THE RS MODEL

Galaxy (1)	log L_B ($L_\odot$) (2)	σ_m (km s^{-1}) (3)	kT (keV) (4)	Abundance (solar) (5)	N_H 10^{21} cm^{-2} (6)	log L_X (ergs s^{-1}) (7)
NGC 720.....	10.3	247	$0.65^{+0.04}_{-0.04}$	$0.14^{+0.07}_{-0.05}$	$0.3^{+0.7}_{-0.3}$	40.6
NGC 1399.....	10.3	310	$1.05^{+0.01}_{-0.02}$	$0.42^{+0.08}_{-0.07}$	$1.1^{+0.0}_{-0.2}$	41.7[a]
NGC 1404.....	10.2	225	$0.66^{+0.03}_{-0.03}$	$0.18^{+0.09}_{-0.05}$	$0.6^{+0.4}_{-0.4}$	40.7
NGC 4374.....	10.6	287	$0.68^{+0.06}_{-0.06}$	$0.11^{+0.07}_{-0.05}$	$1.4^{+0.6}_{-0.7}$	40.8
NGC 4406.....	10.7	250	$0.83^{+0.01}_{-0.01}$	$0.27^{+0.10}_{-0.04}$	$0.9^{+0.2}_{-0.2}$	42.0
NGC 4472.....	10.9	287	$0.93^{+0.02}_{-0.02}$	$0.33^{+0.07}_{-0.05}$	$1.1^{+0.2}_{-0.2}$	41.8
NGC 4636.....	10.5	191	$0.74^{+0.02}_{-0.01}$	$0.28^{+0.07}_{-0.04}$	$0.9^{+0.2}_{-0.1}$	41.7

Col. (1).—Galaxy ID.
Col. (2).—B luminosity (Tully 1988).
Col. (3).—Mean velocity dispersion (Davies et al. 1987).
Col. (4).—Temperature.
Col. (5).—Iron abundance (solar value $=4.68 \times 10^{-5}$).
Col. (6).—Hydrogen column density.
Col. (7).—X-ray luminosity (0.5–10 keV).
[a] The X-ray luminosity for NGC 1399 is for $r < 10'$.

solar, while the hydrogen column density is consistent with the Galactic value. These abundances derived here are systematically different by a factor of 1.5 from those by Awaki et al. (1994), who adopted a different solar iron abundance. The iron abundances listed in Table 1 are consistent with the results obtained by Loewenstein et al. (1994), Mushotzky et al. (1994), and Matsushita et al. (1994), though Loewenstein et al. (1994) did not include the hard component in their spectrum fitting. When the contribution of the ICM is subtracted, the fluxes of the hard components of NGC 1404 and NGC 4374 are consistent with those of other galaxies when scaled with their optical luminosities (cf. Matsushita et al. 1994).

Figures 2 and 3 show the resulting iron abundances as a function of L_X/L_B and temperature, respectively. There is a marginal trend of the iron abundance with both temperature and L_X/L_B. The four galaxies with highest temperature or L_X/L_B ratio appear to have iron abundances $\sim$0.3–0.4 solar, while the three galaxies with lower L_X/L_B ratio have abundances that are even smaller, $\sim$0.1–0.2 solar. Among the galaxies listed in Table 1, four are in common with our *ASCA* analysis (namely, NGC 4374, NGC 4406, NGC 4472, and NGC 4636). The derived ISM iron abundances of NGC 4374, NGC 4406, NGC 4472, and NGC 4636 are 0.1, 0.2, 0.3, and 0.3 solar, respectively. In contrast, the mean stellar iron abundances of these galaxies are 0.9, 0.7, 1.4, and 0.7 solar, respectively. NGC 720, NGC 1399, and NGC 1404 are not listed in Table 1, but judging from the velocity dispersion of these galaxies ($\sigma_m \simeq$ 230–310 km s^{-1}), one can expect their mean stellar iron abundances to be also approximately solar. In addition, according to equation (1), the SN Ia contribution to the ISM iron is at least solar, when the lowest SN Ia rate is assumed (Cappellaro et al. 1993). The iron abundance of ISM should then be at least twice solar, and the discrepancy factor appears to range from $\sim$4 to $\sim$20. It may actually be even larger, considering that stellar abundances in Figure 2 are luminosity- rather than mass-weighted.

We note that the silicate discrepancy, if any, is not as significant as the iron. The silicate abundance can be deter-

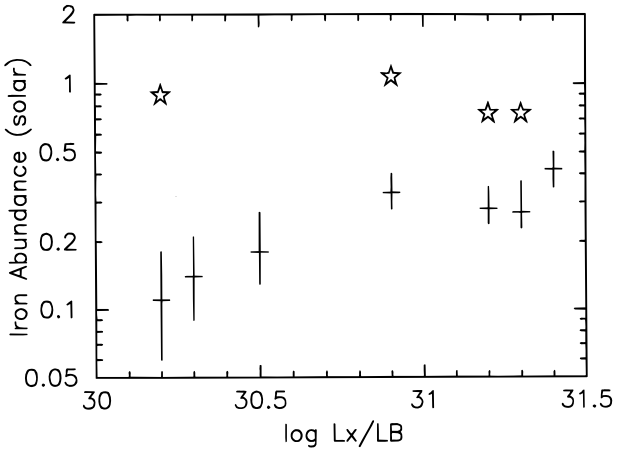

FIG. 2.—Iron abundance of the ISM for the seven elliptical galaxies in our sample (cf. Table 2) determined using the Raymond-Smith model, as a function of L_X/L_B, where L_X is measured for 0.5–10 keV and given in units of ergs s^{-1} and L_B is in solar units. Open stars indicate the mean stellar iron abundances (cf. Table 1).

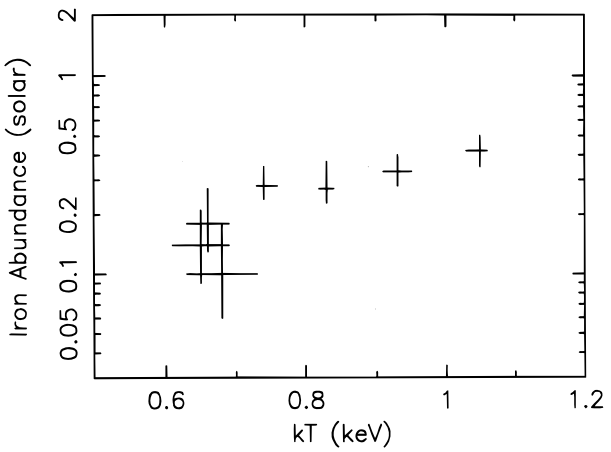

FIG. 3.—Iron abundance of the ISM for the same galaxies as in Fig. 2, as a function of temperature of the ISM, also determined using the Raymond-Smith model.

mined from the silicate K line, and the atomic physics of this He-like Si line are believed to be much secure than the iron L line, although one needs to evaluate precisely the hard component in this energy range. We have estimated the silicate abundance for X-ray luminous ellipticals, NGC 1399, NGC 4406, NGC 4472, and NGC 4636, by using the higher energy parts ($kT \geq 1.7$ keV) of the same spectra. A Raymond-Smith model with the solar abundance ratios is fitted to each galaxy, and a 10 keV bremsstrahlung spectrum is assumed for the hard component. The resulting temperatures are consistent with those given in Table 2 for NGC 4406 ($0.86^{+0.17}_{-0.11}$ keV) and NGC 4636 ($0.78^{+0.10}_{-0.06}$ keV), but slightly higher for NGC 1399 ($1.27^{+0.11}_{-0.11}$ keV) and NGC 4472 ($1.05^{+0.06}_{-0.06}$ keV). The silicate abundance is on average half of solar, or, more precisely, $0.43^{+0.20}_{-0.13}$ solar for NGC 1399, $0.53^{+0.48}_{-0.37}$ solar for NGC 4406, $0.48^{+0.26}_{-0.17}$ solar for NGC 4472, and $0.60^{+1.00}_{-0.17}$ solar for NGC 4636. Recently NGC 4636 was reobserved during *ASCA* run AO4 with an exceptionally long exposure time (200 ks) by T. Ohashi et al. (1996, private communication), and the silicate abundance for this galaxy is now believed to be $1.0^{+0.3}_{-0.3}$ solar. Since the bulk of silicate is synthesized in SN II's and comparatively less is synthesized in SN Ia's, the X-ray abundance of silicate should be nearly equal to the stellar silicate abundance. If the stars' silicate abundance is the same as the iron abundance, this should be about solar; thus the optical and the X-ray silicate abundance are consistent with each other for NGC 4636. For the other three galaxies there is no reason not to expect a similar increase in the measured silicate abundance, once much higher signal-to-noise ratios are achieved in their spectra.

3. ASTROPHYSICAL IMPLICATIONS OF A LOW IRON ABUNDANCE IN THE HOT ISM

A comparison of the iron abundances as inferred from optical observations of the starlight and from X-ray observations of the hot ISM has then revealed a major discrepancy: even neglecting any ISM enrichment from SN Ia's, the stellar iron abundances exceed those derived for the hot ISM by factors that range between ~ 2 and ~ 10 (cf. Tables 1 and 2, and Fig. 2). We believe that the *optical* and the X-ray abundances cannot be easily reconciled, and therefore the existence of this macroscopic discrepancy opens three main options: (1) the optical abundances are seriously in error *and* the SN Ia iron enrichment is much lower than currently believed; (2) there is a problem with the interpretation of the iron L lines; and (3) both optical and X-ray abundances are correct, but the ISM iron is somehow hidden to X-ray observations. In this section we assume the ISM iron abundances inferred from the X-ray observations and reported in § 2.2 to be correct, and explore the astrophysical consequences that stem from that assumption.

The low iron abundances reported for some galaxies (especially NGC 1404 and NGC 4374) require the SN Ia iron enrichment at the present time to be vanishingly small, and the average iron abundances of the stellar component to be in error by a large factor. The first requirement has been extensively discussed in RCDP. Even with a SN Ia rate as low as advocated by Cappellaro et al. (1993), $\vartheta = \frac{1}{4}$, SN Ia's would enrich the ISM to well above solar if each SN Ia releases 0.7 $M_\odot$ of iron. Thus, the implications of option 1 for SN Ia's include a drastic reduction of the SN Ia rate in ellipticals over the most conservative estimates, and/or a drastic reduction of the iron yield per SN Ia over current theoretical estimates. In practice, X-ray observations imply that the product $\vartheta_{SN}(M^{Fe}/0.7\ M_\odot)$ should be much less than $\sim \frac{1}{4}$, thus challenging at once both the theory and the observations of SN Ia's.

Concerning the stellar abundances, we note that the existing Mg_2-[Fe/H] calibrations are far from being exempt from uncertainties, since they are based on elaborate synthetic population modeling and might be in error for a variety of reasons. Moreover, the Mg_2 index is a rather indirect measure of iron abundance, while the [Mg/Fe] ratio may not be solar in the stellar component of elliptical galaxies, with Mg being enhanced compared to Fe by perhaps as much as a factor of ~ 2 (e.g., Worthey, Faber, & González 1992; Davies et al. 1993). If so, the discrepancy could be somewhat alleviated but clearly not removed. Again, a combination of an erroneous Mg_2-[Fe/H] calibration and an underestimate of the metallicity gradients within galaxies should be required to explain the much larger iron abundances inferred from optical observations compared to those derived from the X-ray data. We believe this to be a very drastic requirement, and emphasize that it would have a major impact on the stellar population studies of elliptical galaxies, and therefore on our understanding of their formation and evolution.

3.1. *Type Ia Supernovae and Gas Flows in Elliptical Galaxies*

The drastic reduction in the rate of SN Ia's demanded by the X-ray data has major implications for the interpretation of the X-ray properties and evolution of elliptical galaxies. With $\vartheta_{SN} \ll \frac{1}{4}$, the SN heating of the ISM becomes virtually negligible for the dynamics of the gas flows in these galaxies at the present time. In the absence of alternative internal sources of heat, the ISM of virtually all elliptical galaxies would now be in a cooling flow regime. Accordingly, all elliptical galaxies should be very bright in X-rays, at variance with the observations that indicate a large dispersion in X-ray luminosity for a given optical luminosity (Canizares et al. 1987; Donnelly, Faber, & O'Connell 1990; Ciotti et al. 1991; Fabbiano, Kim, & Trinchieri 1992; Renzini 1996b). With sufficient SN heating instead, most galaxies are in a wind or outflow regime, with substantially lower X-ray luminosity compared to inflow models. To account for the X-ray luminosity dispersion even in the absence of SN heating, an alternative heating source seems to be required in order to maintain the majority of ellipticals in a wind or outflow regime at the present time. This may be represented by sporadic AGN activity triggered each time that a central cooling catastrophe turns the gas flow from an outflow to an inflow regime, thus fueling a previously starving central black hole (Ciotti et al. 1991; Binney & Tabor 1995; Ciotti & Ostriker 1996; see also Renzini 1994a, 1996b). Alternatively, it has been suggested that ram pressure stripping may be responsible for the partial or total removal of the hot ISM in some galaxies, thus reducing the amount of X-ray–emitting gas and X-ray luminosity by appealing to environmental effects (White & Sarazin 1991). This explanation would predict elliptical galaxies in the Coma Cluster to be on average fainter in X-rays than ellipticals in Virgo of similar optical luminosity, a result of the somewhat higher ram pressure in Coma compared to Virgo. However, *ROSAT* observations of individual galaxies in the Coma Cluster do not reveal systematic differences with respect to those in Virgo (Dow & White

1995), which argues against strong environmental effects being responsible for the X-ray luminosity dispersion among galaxies in these two clusters.

In conclusion, if one excises SN Ia's from the factors affecting gas flows in today's ellipticals, alternative mechanisms capable of driving gas out of galaxies have to take their place on the stage. A prime candidate is sporadic (or recurrent) AGN activity, although ram pressure stripping cannot be fully excluded at the present time.

3.2. *SN Ia Rate in the Past*

Over the last 15 years the notion of a prime role of SN Ia's in the production of iron in the Galaxy has become widely accepted. The basic fact is represented by the O/Fe ratio and ratios of α-elements to iron in metal-poor stars of the Galactic halo, which is 3–4 times solar (Sneden, Lambert, & Whitaker 1979; Gratton & Ortolani 1986; Bessell, Sutherland, & Ruan 1991; Barbuy 1992; see also the review by Wheeler, Sneden, & Truran 1989). The interpretation of the observed trend of [α/Fe] versus [Fe/H] is based on the different nucleosynthesis yields and timescales of SN Ia's and SN II's, with the enrichment of the halo being sufficiently rapid to sample almost exclusively the prompt release of SN II products (primarily the α-elements, such as O, Ne, Mg, Si, etc., but comparatively little iron), while it takes a longer time for SN Ia's to release the bulk of their iron (e.g., Sneden et al. 1979; Greggio & Renzini 1983a, 1983b; Matteucci & Greggio 1986; Abia, Canal, & Isern 1991; Matteucci & François 1992; Timmes, Woosley, & Weaver 1995; Greggio 1996; Ruiz-Lapuente, Burkert, & Canal 1996). In this scenario, to which we refer as the Standard Chemical Model (SCM), SN II's had produced virtually all the iron now locked in extreme Population II stars, while at later times SN Ia's would have taken the lead as main iron producers, to the extent that $\sim\frac{3}{4}$ of the iron present in the sun would come from SN Ia's (Timmes et al. 1995 prefer $\sim\frac{1}{2}$). Additional support to the SCM comes from star-forming (spiral) galaxies exhibiting a SN Ia rate about $\frac{1}{3}$ that of all other types together (Cappellaro et al. 1993). If each SN Ia produces ~ 10 times more iron than other SNs, as currently believed, then the present iron production rate in spiral galaxies is indeed dominated ~ 3 to 1 by SN Ia's (see RCDP).

The SCM has a series of testable predictions when applied to elliptical galaxies and clusters of galaxies, if one assumes that IMF and SN Ia productivity are the same as in our own Galaxy. The first prediction is that the past time-averaged SN Ia rate in ellipticals had to be much higher than the present rate, otherwise SN Ia's would have produced a negligible fraction of all the iron that is observed in clusters of galaxies (Ciotti et al. 1991; Arnaud et al. 1992; RCDP). More quantitatively, with $\vartheta_{\rm SN} = 1$ such an average rate should be ~ 10 times higher than the present rate in ellipticals in order for SN Ia's to have produced $\sim\frac{3}{4}$ of the iron that is observed in clusters. A reduction of the present rate by, e.g., a factor of 4 (i.e., to $\vartheta_{\rm SN} = \frac{1}{4}$) does not necessarily invalidate this scenario, if the past average rate is increased by the same factor. In the frame of the parameterization mentioned in § 1, this would require increasing the slope s from ~ 1.4 to ~ 1.7. This is not at all inconceivable, given our enduring ignorance of the nature of SN Ia progenitors (Renzini 1996a; Branch et al. 1995).

In this context, it is worth emphasizing that the present iron abundance in the ISM of ellipticals can effectively constrain only the recent SN Ia rate, as—with the exception of a few extreme cases (Loewenstein & Mathews 1991)—the flow time of the gas in or out of the galaxy is just a few Gyr (Ciotti et al. 1991). In particular, no constraint is placed on the first ~ 10 Gyr, when indeed SN Ia's would have delivered most of their iron yield. We conclude that a moderately low iron abundance in the ISM of today's ellipticals is certainly a challenge, but does not necessarily invalidate the applicability of the SCM also to elliptical galaxies.

3.3. *Enrichment of the Intracluster Medium*

3.3.1. *Iron Content of Galaxy Clusters*

In this section we explore further consequences of a low iron content of elliptical galaxies that may be relevant for our understanding of the chemical and thermal evolution of the ICM.

A very effective way of quantifying the iron content of clusters is by their iron mass-to-light ratio (IMLR), i.e., by the ratio of the total mass of iron in a cluster to the total optical luminosity of the cluster galaxies. The IMLR can be defined separately for the ICM, for the galaxies themselves, as well as for the cluster as a whole. The IMLR for the ICM of clusters appears to be remarkably constant, irrespective of the cluster optical luminosity (RCDP; see Fig. 1 of Renzini 1994b):

$$\left(\frac{M^{\rm Fe}}{L_B}\right)^{\rm ICM} \simeq (0.01 - 0.02) h_{50}^{-1/2} \frac{M_\odot}{L_\odot}\,, \qquad (9)$$

The IMLR for the iron now locked into stars inside cluster galaxies is given by

$$\frac{M_*^{\rm Fe}}{L_B} = \langle Z_*^{\rm Fe}\rangle \frac{M_*}{L_B} \simeq (0.01 - 0.02) \frac{\langle Z_*^{\rm Fe}\rangle}{Z_\odot^{\rm Fe}} h_{50} \frac{M_\odot}{L_\odot}\,, \quad (10)$$

where $\langle Z_*^{\rm Fe}\rangle$ is the average iron mass fraction in the stellar component of cluster galaxies, and M_*/L_B is the stellar mass-to-light ratio of galaxies. A comparison between equation (9) and equation (10) reveals that—assuming the average stellar iron to be solar—there is nearly the same amount of iron in the ICM as there is locked into stars (for $h_{50} = 1$). This *fifty-fifty* condition has been extensively discussed. Note that the total IMLR is not very sensitive to the adopted value of the Hubble constant, but the relative share of iron between the two cluster components shows a significant dependence (Renzini 1994b). For example, with $h_{50} = 2$ the fifty-fifty share turns to a 3 to 1 share in favor of galaxies, i.e., the ICM holds $\sim\frac{1}{4}$ of the total ion, cluster galaxies $\frac{3}{4}$. The iron share betweeen the two cluster components sets a strong constraint on models of galaxy formation and evolution: nearly as much iron needs to be ejected from galaxies as remains locked into stars.

These figures assume $\langle Z_*^{\rm Fe}\rangle \simeq Z_\odot^{\rm Fe}$. Now, if the abundances derived from the X-ray data are correct, the average metallicity of stars is appreciably below solar. To illustrate the impact of the new abundances, we take for $\langle Z_*^{\rm Fe}\rangle$ the straight average of the values in Table 2, i.e., ~ 0.2 times solar. With this value equation (10) gives a stellar IMLR $\sim\frac{1}{5}$ that of the ICM, i.e., $\sim\frac{5}{6}$ of the total iron is now in the ICM and only $\frac{1}{6}$ remains in stars. Thus, the iron abundances from the X-ray data imply a much more dramatic degassing of galaxies, which should have lost perhaps more than 80% of their initial mass. Such rather extreme conse-

quences can be partly alleviated by appealing to a shorter extragalactic distance scale: with $h_{50} = 2$ the iron share becomes ~ 2 in 1 in favor of the ICM, with galaxies having lost $\sim 60\%$ of their initial mass. In conclusion, the low iron abundances in the ISMs of ellipticals that are indicated by the X-ray data have profound implications for the formation process of galaxies, dramatically altering the mass budget, i.e., the ratio of the (baryonic) mass ejected by galaxies in the course of their formation and evolution, to the residual galaxy mass (in stars).

This argument can be followed a little further. We take the Coma Cluster as a representative rich cluster. The total mass of the ICM is estimated to be $\sim 3.1 \times 10^{14}\, h_{50}^{-5/2}\, M_\odot$ and the total stellar mass in galaxies $\sim 2.0 \times 10^{13}\, h_{50}^{-1}\, M_\odot$ (White et al. 1993). Thus the ICM-to-star mass ratio is ~ 15 to 1 for $h_{50} = 1$, or ~ 5 to 1 for $h_{50} = 2$. Thus, the fraction of the ICM that comes from galaxies is about $\frac{1}{3}$, irrespective of h_{50}, with the residual $\frac{2}{3}$ being represented by pristine material, never incorporated into galaxies. In the traditional view instead, with $\langle Z_*^{\rm Fe} \rangle \simeq Z_\odot^{\rm Fe}$, only a much smaller fraction of the ICM, i.e., $\sim 1/15$, was once incorporated into galaxies.

3.3.2. *Heating of the ICM*

The presence of a large amount of iron in the ICM implies that a large amount of matter has been lost by galaxies. Arguments are presented in RCDP supporting the notion that matter was ejected rather than swept by ram pressure stripping, as also indicated by the IMLR of the ICM being independent of cluster richness. Thus, along with mass, galaxies have also injected kinetic energy (i.e., heat) into the ICM. The kinetic energy associated to galactic winds, again per unit cluster light, is given by one-half the ejected mass times the square of the typical wind velocity (e.g., Renzini 1994b), i.e.,

$$\frac{E_w}{L_B} = \frac{1}{2}\left(\frac{M^{\rm Fe}}{L_B}\right)^{\rm ICM}\left\langle \frac{v_w^2}{Z_w^{\rm Fe}} \right\rangle \simeq 1.5 \times 10^{49}\, \frac{1}{Z_w^{\rm Fe}/Z_\odot^{\rm Fe}} \left(\frac{v_w}{500\ {\rm km\ s^{-1}}}\right)^2 \frac{\rm ergs}{L_\odot}, \quad (11)$$

where the empirical IMLR for the ICM has been used (with $h_{50} = 1$), and $Z_w^{\rm Fe}$ is the average metallicity of the winds. In wind models for elliptical galaxy formation (e.g., Arimoto & Yoshii 1987) galactic winds are established at the culmination of the metal enrichment process, and their metallicity is about 3 times the average stellar metallicity. Therefore, by decreasing $\langle Z_*^{\rm Fe} \rangle$ by a factor of 5, $Z_w^{\rm Fe}$ is also seemingly decreased, and the resulting galactic wind heating of the ICM is increased by the same factor.

Galactic wind heating has great importance for the evolution of the ICM, and therefore for the X-ray evolution of clusters of galaxies (Kaiser 1991; Cavaliere, Colafrancesco, & Menci 1993; Metzler & Evrard 1994). Here we just emphasize that a reduction of the estimated metallicity of stars in ellipticals automatically implies an increase by the same factor in the estimated heating of the ICM.

3.3.3. *Failure of the Standard Chemical Model?*

Further challenge to the SCM comes from *ASCA* observations of the ICM in several clusters of galaxies. Preliminary results appear indeed to indicate an enhancement of the α-elements (notably neon) relative to iron in the ICM, which argues for a dominant SN II enrichment (Mushotzky 1994; Mushotzky et al. 1996). When applied to a cluster as a whole, the SCM predicts near-solar α/Fe ratios when the total mass of each element is considered, i.e., the total amount locked in stars within galaxies plus the amount diffused in the ICM (RCDP). The model also predicts an α-element enhancement compared to iron in the stellar component of galaxies, and instead an α-element depletion in the ICM. This *chemical asymmetry*—the signature of the SCM—follows from the promptly released SN II products being predominantly locked into stars during the intense star-forming activity at the formation epoch of ellipticals, while a main fraction of the total iron—more slowly released by SN Ia's—flows out of galaxies into the ICM after galactic winds are established and most star formation has ceased. As already mentioned, optical data suggest that Mg is indeed enhanced in the stellar component of ellipticals, which is in agreement with the expectations from the SCM. However, the enhanced [α/Fe] ratio in the ICM of several clusters (up to ~ 2 times solar according to Mushotzky et al. 1996) appears at variance with that predicted by the SCM, although a reconciliation might not be completely impossible (Loewenstein & Mushotzky 1996; Ishimaru & Arimoto 1997).

In summary, the abundances derived from X-ray data relative to the ISM of individual ellipticals require SN Ia's to be irrelevant at the present time, and the X-ray–derived abundance ratios for the ICM require SN Ia's to have been irrelevant in the past. In other words, all X-ray data appear consistent with the notion that all elements in clusters of galaxies, including iron, are produced by SN II's with a negligible contribution from SN Ia's (see also Loewenstein & Mushotzky 1996). Thus the SCM dramatically fails to account for the chemical abundances as derived from the X-ray observations.

The production of all the iron that is observed in clusters of galaxies may indeed be produced by SN II's alone, provided that the IMF is somewhat flatter than in the solar neighborhood, and an IMF slope $x \simeq 0.9$ would be sufficient for this purpose (Ciotti et al. 1991; Arnaud et al. 1992; RCDP; Matteucci & Gibson 1995). A variant of this scenario appeals to bimodal star formation, with the starburst activity in early ellipticals generating only stars more massive than ~ 2 or 3 $M_\odot$, as advocated by Arnaud et al. (1992) and Elbaz, Arnaud, & Vangioni-Flam (1995).

3.3.4. *Suppressing Binary Star Formation in Ellipticals?*

There are therefore viable alternatives to SN Ia's for the production of all the iron that is observed. This is not the question. The question is instead why SN Ia's should play a major role within the Galaxy and yet be irrelevant in the ecology of ellipticals and clusters of galaxies. This indeed requires SN Ia's to be selectively suppressed in the stellar populations of clusters of galaxies (ellipticals) with respect to spirals. This embarrassing implication is discussed next.

SN Ia's are believed to be the product of binary star evolution, in which a white dwarf accretes material from a companion until a thermonuclear runaway is ignited in the white dwarf. Suppressing by a great factor SN Ia's in elliptical compared to spiral galaxies therefore translates into suppressing binary star formation by nearly the same factor. Binary star frequency in ellipticals can be estimated in two ways. As already mentioned, the hard spectral component is generally ascribed to a population of low-mass

X-ray binaries (LMXRB's), and there appears to be no shortage of such objects in elliptical galaxies, since the ratio of the X-ray luminosity of the hard component to the optical luminosity is the same as in spirals (Canizares et al. 1987; Pellegrini & Fabbiano 1994; Pellegrini 1994; Matsushita et al. 1994).

Another manifestation of binaries is represented by nova outbursts. In Virgo ellipticals the frequency of novae per unit galaxy light is the same as in nearby spirals (Della Valle et al. 1994). Again, this argues for the binary frequency in ellipticals being the same as in spirals. We conclude that the option of a drastically suppressed binary star formation in ellipticals does not find independent support. Apparently, suppression should apply only to the particular kind of binary systems that are capable of triggering an SN Ia event. SN Ia precursors belong certainly to different kinds of binaries than LMXRBs or novae. LMXRBs contain a neutron star, i.e., had a massive-star primary. Novae have a white dwarf primary and an unevolved low-mass secondary. In SN Ia precursors, instead, the secondary component must also have evolved away from the main sequence. Although a difference exists after all, it is hard to find arguments supporting a selective suppression of just those binaries with a primary star less massive than $\sim 8\,M_\odot$ and a secondary star more massive than $\sim 0.8\,M_\odot$, while keeping unchanged the productivity of other binaries. The first limit ensures that the primary will become a white dwarf, the second one that the secondary will evolve off the main sequence in less than ~ 15 Gyr. We conclude that SN Ia precursor–binary star suppression offers a formal solution to the dilemma, but a very contrived one indeed.

It is worth emphasizing that bimodal star formation does not solve the problem. If most of the metals in clusters of galaxies are produced in early starbursts where only stars more massive than $\sim 2\,M_\odot$ are formed (Arnaud et al. 1992), then this starburst population will also include all the SN Ia precursors as well. The total mass of the binary SN Ia precursors is in fact in the range from ~ 4 or $5\,M_\odot$ up to $\sim 16\,M_\odot$, with a mass of the primary in the range between ~ 3 to $\sim 8\,M_\odot$, irrespective of the specific SN Ia model (Greggio & Renzini 1983a; Iben & Tutukov 1984). Indeed, there appears to be no way of triggering a destructive thermonuclear explosion in binaries with initial total mass below $\sim 4\,M_\odot$. Bimodal star formation models for the chemical enrichment of clusters of galaxies explicitly assume that only stars with $M \gtrsim 2\,M_\odot$ are formed during early bursts, but in addition implicitly assume the binary progenitors of SN Ia's to be completely suppressed in the burst population. Formally, this extra assumption could be avoided if the burst population were to produce only individual stars more massive than $\sim 8\,M_\odot$, either single or in a binary. If so, the population would not produce carbon-oxygen white dwarfs at all, and the necessary objects to make SN Ia's would be absent in the population. Given the arbitrary nature of the bimodal star formation hypothesis, and in particular of the value of the lower mass cutoff, an assumption of this kind is certainly not less legitimate than others; it would actually have the advantage of avoiding the ad hoc assumption of the binary suppression in the burst population.

A simple chemical evolution model can be used if SN Ia's are indeed irrelevant in the iron budget of ellipticals and clusters. In this case, in the closed-box approximation the chemical evolution of an elliptical galaxy is well described by

$$\langle Z_*^{\rm Fe}\rangle = y^{\rm Fe} - \frac{M_{\rm gas} Z_{\rm gas}^{\rm Fe}}{M_*}\,, \tag{12}$$

where $y^{\rm Fe}$ is the *yield* of iron produced by each stellar generation, and $M_{\rm gas}$ and $Z_{\rm gas}^{\rm Fe}$ represent respectively the mass and iron content of the ISM at any given time (e.g., Tinsley 1980). Therefore, when a wind is established, the amount of iron that is ejected ($M_{\rm gas} Z_{\rm gas}^{\rm Fe}$) can be obtained by this relation, and the resulting IMLR of the ICM turns out to be

$$\left(\frac{M_{\rm SN\,II}^{\rm Fe}}{L_B}\right)^{\rm ICM} = (y^{\rm Fe} - \langle Z_*^{\rm Fe}\rangle)\,\frac{M_*}{L_B}\,. \tag{13}$$

In this purely chemical framework, a low iron abundance in the stellar component helps to produce a higher IMLR in the ICM, since a larger fraction of the iron yield remains available for ICM enrichment after star formation has ceased. Following Nomoto et al. (1993), we adopt the iron yield $y^{\rm Fe}$ by massive stars as $1.4\,Z_\odot^{\rm Fe}$ for $x = 1.05$ and $0.21\,Z_\odot^{\rm Fe}$ for $x = 1.50$. Again we recover the result that a fairly flat IMF ($x \lesssim 1$) is required to account for the iron in the ICM, while no iron at all would be left for polluting the ICM in the case $x \gtrsim 1.5$, even if the iron abundance in stars is as low as 0.2 solar. We recall that a flat IMF would also help in producing synthetic stellar populations as red as the observed ellipticals (Arimoto & Yoshii 1987).

4. WAYS OF HIDING IRON FROM X-RAY OBSERVATION

So far we have assumed that the iron ejected by mass-losing stars and SNs is neither further diluted nor astrated from the ISM. This is equivalent to assuming that the abundance indicated by equation (1) is indeed the one to be compared to the ISM abundance measured from X-ray observations. This assumption is now relaxed in the attempt to explore whether a solution to the iron discrepancy can be found in this direction.

4.1. *Is Iron Mostly in Flakes?*

When comparing the predicted abundance from equation (1) to abundances derived from X-ray observations, one implicitly assumes that all the iron ejected by stars and SN Ia's is now in the gas phase of the ISM. Actually, it is likely that some fraction of the iron condenses into dust grains (or *iron flakes*) while it is in the circumstellar envelope of mass-losing red giants, and remains locked in them for some time after ejection. Indeed, along with other refractory elements, iron appears to be depleted in planetary nebulae by factors up to ~ 100 (Clegg 1989). Seemingly, part of the fresh iron synthetized by SN Ia's could also condense into solid particles when heating from the Ni and Co radioactive decay has sufficiently declined. Such solid iron could join the hot ISM phase only after sputtering has dissolved the grains.

While there is little doubt that at least a fraction of the iron is injected in the form of solid particles, the question is whether iron remains in a solid phase for a time long enough to account for the iron discrepancy. The time required to evaporate 90% of the iron particles in a 10^7 K plasma is $\sim 10^5/n_e$ yr cm^{-3} (Itoh 1989). Electron densities in the ISMs of ellipticals range from $\sim 10^{-1}$ near the center to $\sim 10^{-3}$ several effective radii away, and therefore evaporation times range from 10^6 to 10^8 yr. This compares to a

flow time of a few Gyr, and we conclude that only a tiny fraction of iron could be hidden in dust particles, thereby subtracting itself in X-ray observations.

4.2. *Or in Super Iron-rich Jupiters?*

Here we mention yet another, admittedly exotic solution to the iron discrepancy. Thermal instabilities causing a fraction of the gas to drop out of the flow locally have often been invoked as the ultimate depository for both cluster and galaxy inflows (e.g., Fabian et al. 1986; Sarazin 1986). Together with this hypothesis comes the additional conjecture that such instabilities would lead to the formation of low-mass, unobservable objects such as lower–main-sequence stars, brown dwarfs, or "jupiters." This scenario is far from having been supported by independent observations, while it has encountered several physical difficulties (e.g., Murray & Balbus 1992; Kritsuk 1992). Here we just adopt it as a working hypothesis.

The sites of SN Ia explosions remain as local enhancement of the iron abundance before Rayleigh-Taylor instabilities and mixing homogenize the ISM. It has been suggested that such inhomogeneities may work as seeds for the growth of local thermal instabilities, thanks to their high iron enhancement causing more efficient cooling (Mathews 1990). Therefore, one may speculate that most of the iron released by SN Ia's could ultimately be disposed of in the dark residual of the thermal instabilities, e.g., in super–iron-rich jupiters, rather than enriching the ISM and the ICM.

By good fortune, this scenario has one testable prediction. Local thermal instabilities—if they exist—should be more efficient in dropping SN Ia products out of the flow near the center where the cooling time is short, compared to the outer regions. Thus, iron should be preferentially depleted near the center, and a positive abundance gradient should develop. Actual observations seem in any case to indicate the opposite gradient, with iron being more enhanced near the center (Mushotzky et al. 1994). We conclude that hiding iron in jupiters does not appear to be a viable solution to the discrepancy.

4.3. *Is the ISM Diluted by the ICM?*

Equation (1) assumes that the whole ISM in a galaxy is made of materials that have been lost by the stellar component of the galaxy itself. Elliptical galaxies are often embedded in a hot ICM, and ICM materials can be accreted if an inflow is established, thus diluting the indigenous ISM (RCDP). For the specific case of NGC 1399 (the cD galaxy in the Fornax Cluster) RCDP's detailed flow modeling indicates that a dilution by up to a factor of 3 is possible, thus easing the discrepancy somewhat. RCDP also argue that some dilution may be effective in the case of NGC 4472, that is, part of a subcondensation within the Virgo Cluster.

The hypothesis that accretion from the ICM and dilution are responsible for the iron discrepancy has some testable consequences. The first is that accreting galaxies should be overluminous in X-rays, as the additional $P\,dV$ work on the infalling material needs to be radiated away in a quasi-stationary cooling flow. NGC 1399 is in fact somewhat more luminous than expected from an isolated inflow regime (RCDP), which apparently supports the dilution hypothesis. However, one expects iron dilution to be more effective in galaxies that are located in a cluster or group with a dense ICM, and less effective in isolated ellipticals, which are not projected on a high X-ray surface brightness environment. Among the galaxies in Table 2, some are member of the Virgo Cluster—and dilution may be invoked—but others (e.g., NGC 4636 and NGC 720) are isolated and in a low-density environment. Yet the iron abundance in the latter galaxies is as low as, or even lower than, that of cluster members. We conclude that dilution does not offer a viable solution either.

5. IRON L DIAGNOSTICS

5.1. *XSPEC versus Meka versus Masai*

The abundances reported in § 2.2 have been obtained from the standard RS thin-plasma emission model incorporated in the XSPEC package, and in this section we compare these results with those obtained using the so-called Meka model (Mewe, Gronenschild, & van den Oord 1985; Mewe, Lemen, & van den Oord 1986; Kaastra 1992) and Masai model (Masai 1984). Such models use somewhat different input physics, e.g., ionization, collisional excitation and recombination rates, energy levels, and equivalent widths. At $T \simeq 1$ keV, iron ions have still several bound electrons, and therefore spectra of the iron L line blend are very complex. Features of the iron L blend can differ considerably in different models, and so do the resulting iron abundances.

Apart from the use of different models, we then proceeded in exactly the same way as described in § 2.2. For the solar iron abundance we have used 4.68×10^{-5} by number for all models, and the results are shown in Table 3 and Figure 4. The physical parameters obtained by these models are quite different. Temperatures derived from the Meka model are about 0.2 and 0.15 keV lower than those derived from the RS model and the Masai model, respectively. The iron abundance can differ sometimes by a factor of 2–3 from model to model. The Meka model gives iron abundances similar to that of the RS model, except for NGC 1399, for which the Meka model gives a slightly lower iron abundance. We note that the RS model gives the highest temperature for this galaxy. The Masai model gives systematically larger iron abundance than the RS model.

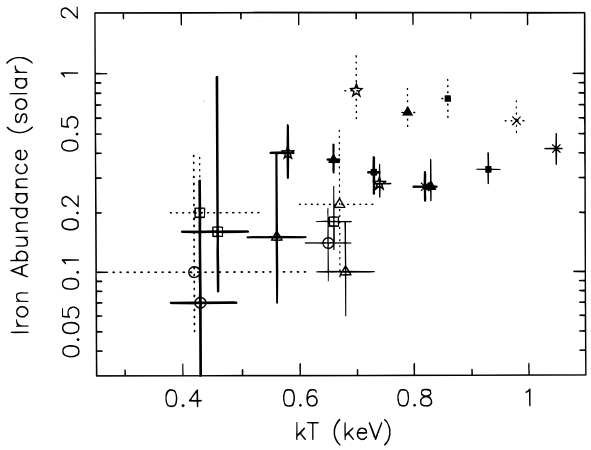

FIG. 4.—Iron abundances of the ISM for the same seven galaxies as in Figs. 2 and 3, as a function of the ISM temperature. Solid, solid thick, and dotted error bars indicate values obtained by the Raymond-Smith model, Meka model, and Masai model, respectively. Individual galaxies are identified by the same symbol at the center of the error bars.

TABLE 3

IRON IN THE HOT ISM OF ELLIPTICAL GALAXIES FROM THE MEKA AND MASAI MODELS

	MEKA			MASAI		
MODEL GALAXY (1)	kT (keV) (2)	Abundance (solar) (3)	N_H (10^{21} cm^{-2}) (4)	kT (keV) (5)	Abundance (solar) (6)	N_H (10^{21} cm^{-2}) (7)
NGC 720.....	$0.43^{+0.06}_{-0.05}$	$0.07^{+0.22}_{-0.04}$	$1.3^{+1.1}_{-1.3}$	$0.42^{+0.20}_{-0.14}$	$0.10^{+0.30}_{-0.05}$	$1.0^{+1.0}_{-1.0}$
NGC 1399.....	$0.82^{+0.02}_{-0.02}$	$0.27^{+0.05}_{-0.04}$	$1.5^{+0.2}_{-0.2}$	$0.98^{+0.02}_{-0.02}$	$0.58^{+0.16}_{-0.08}$	$1.1^{+0.2}_{-0.2}$
NGC 1404.....	$0.46^{+0.05}_{-0.06}$	$0.16^{+0.80}_{-0.08}$	$1.4^{+1.0}_{-1.4}$	$0.43^{+0.10}_{-0.05}$	$0.20^{+0.20}_{-0.10}$	$1.6^{+1.5}_{-0.6}$
NGC 4374.....	$0.56^{+0.06}_{-0.05}$	$0.15^{+0.25}_{-0.08}$	$1.5^{+0.8}_{-0.7}$	$0.67^{+0.06}_{-0.06}$	$0.22^{+0.30}_{-0.13}$	$1.1^{+0.6}_{-0.6}$
NGC 4406.....	$0.66^{+0.01}_{-0.01}$	$0.37^{+0.07}_{-0.05}$	$1.0^{+0.1}_{-0.2}$	$0.79^{+0.02}_{-0.01}$	$0.64^{+0.20}_{-0.10}$	$0.6^{+0.2}_{-0.2}$
NGC 4472.....	$0.73^{+0.01}_{-0.01}$	$0.32^{+0.06}_{-0.07}$	$1.5^{+0.2}_{-0.2}$	$0.86^{+0.01}_{-0.01}$	$0.75^{+0.20}_{-0.15}$	$0.7^{+0.2}_{-0.2}$
NGC 4636.....	$0.58^{+0.01}_{-0.03}$	$0.40^{+0.15}_{-0.10}$	$1.1^{+0.2}_{-0.2}$	$0.70^{+0.01}_{-0.02}$	$0.82^{+0.46}_{-0.23}$	$0.5^{+0.2}_{-0.3}$

Col. (1).—Galaxy ID.
Col. (2).—Temperature (Meka model).
Col. (3).—Iron abundance (Meka model).
Col. (4).—Hydrogen column density (Meka model).
Col. (5).—Temperature (Masai model).
Col. (6).—Iron abundance (Masai model).
Col. (7).—Hydrogen column density (Masai model).

For the three X-ray–luminous galaxies in Virgo (NGC 4406, NGC 4472, and NGC 4636) the abundances are almost solar. Even the Masai model, however, gives abundances $\sim$0.2–0.3 times solar for NGC 720, NGC 1404, and NGC 4374, with an upper limit of $\sim$0.6 solar.

In conclusion, the size of the iron discrepancy is somewhat reduced, but by no means eliminated, when adopting iron abundances from the Masai model. This is especially so when allowance is made for the iron enrichment by SN Ia's.

5.2. *The Iron* L *Problem*

The iron L blends contain a few hundred lines produced by several ionization stages, and the specific blends depend on temperature. The atomic physics of such multielectron ions is rather complicated, hence affected by uncertainties that are difficult to quantify but may be rather large. Atomic data such as ionization, recombination, and especially collisional excitation rate coefficients are still controversial, which accounts for the differences among the various models. New calculation of plasma spectra using new atomic data (Liedahl, Osterheld, & Goldstein 1995) show that the total power of the iron L shell lines can be up to 40% different from that in the Meka model, even using the same ionization and recombination rates. The temperatures explored in this study ($kT \geq 1.2$ keV) are more pertinent to galaxy groups and clusters, where problems with the iron L diagnostics have also been encountered (Fabian et al. 1994), and therefore one cannot firmly exclude even larger discrepancies at the lower temperatures that are typical of elliptical galaxies.

As shown in the previous section, the derived abundances from different models may differ by a factor of 2 or 3. When spectra are fitted, besides abundance the fit parameters include two plasma temperatures, the strengths of these two components, and the hydrogen column density of the cold gas absorbing soft X-rays. The procedure is therefore much more complicated than a simple isothermal plasma model, and so is the circulation of the errors affecting the derived abundance.

To assess the dependence of the resulting abundance on the model ingredients we have calculated spectra of an isothermal plasma with *half* solar abundance using the RS model, convolved them with the *ASCA* response, and then fitted the resulting spectra with isothermal Meka and Masai models. Photoelectric absorption was not included in this exercise. When $kT \gtrsim 1$ keV or $\lesssim 0.5$ keV, all models agree fairly well, but for $0.5 \lesssim kT \lesssim 1$ the abundances from Meka and Masai models are larger by factors of 1.4 and 1.8, respectively, than those from the RS model. For example, for a $kT = 0.9$ keV RS spectrum the abundances from the Meka and Masai models are 0.7 and 0.9 solar, respectively.

It is worth tracing the origin of these differences. The excitation rate of iron levels is the same in the Masai and Meka models, while differences exist in oscillator strengths, branching ratios, and especially ionization and recombination rates. When the same ionization and recombination rates are used, the calculated spectra of these two models are almost identical, with differences of at most $\sim$30% for some strong lines. However, when spectra simulated with the Meka model are fitted with the Masai model, the latter gives abundances which are a factor of $\sim$1.5 larger than those in the Meka model. Much larger differences are encountered in more complex situations, e.g., for two-temperature plasmas including photoelectric absorption.

The accuracy of the iron abundances obtained from the iron K complex at $kT \simeq 6.7$ keV is generally much higher than that of abundances from the iron L complex, because the atomic physics is much simpler for the hydrogen-like and helium-like configurations producing the iron K blend. So, when both iron K and iron L features are sufficiently strong in a given object, abundances from the iron K lines can be used to assess the accuracy of the iron L diagnostics. Unfortunately, for $kT \simeq 1$ keV the iron K lines are very weak and cannot be detected, but for $kT \simeq 2$–3 keV both the iron L and iron K lines are detectable. This is the case for the ICM of the Virgo Cluster, and we have analyzed the *ASCA* X-ray spectrum (from the GIS detector) of a nearly isothermal region about 10′ from the center of M87. The isothermal RS model indicates $kT \simeq 3$ keV and an iron abundance $\sim$0.3 solar for this region. When the spectral range around the iron K complex is excluded from the fit, the RS model gives $kT = 2.89 \pm 0.07$ keV and an iron abundance (now determined only from the iron L lines) 0.41 (0.34–0.50) solar. Excluding the spectral range below 1.8

keV, the model gives $kT = 2.90 \pm 0.1$ keV and an iron abundance (now determined only from the iron K complex) 0.40 (0.34–0.47) solar. Thus, for $kT \simeq 3$ keV the iron K and iron L iron abundances agree fairly well. However, this does not ensure the adequacy of the current iron L diagnostics at lower temperatures, since for $kT \lesssim 1$ keV the iron L lines are produced by iron ions in lower ionization stages, hence by completely different transitions, and the atomic physics involved is correspondingly much more complicated, hence more uncertain. Meanwhile, at such low temperatures the iron K complex disappears and no comparison between iron K and iron L diagnostics is possible.

Besides possible systematic errors due to the atomic physics ingredients, the derived iron abundances may also be compromised by the assumption of an isothermal ISM. SN Ia ejecta could be hidden as an unmixed superhot phase in the ICM. When this assumption is relaxed, and a multitemperature ISM is allowed, the derived iron abundances may differ considerably (Fabbiano 1995). To explore this effect, the spectra of the seven galaxies in Table 2 have been fitted with a two-temperature RS model plus a hard component representing the LMXRB contribution, assuming the abundance of each ISM phase to be the same. The resulting temperatures of the two components cluster around $kT \simeq 0.3$ and 1 keV, and the derived iron abundances increase by at most $\sim 30\%$–40%, while the reduced χ^2 does not decrease much except for NGC 4406 and NGC 4636. All in all, the derived iron abundances remain below solar. We conclude that ISM temperature inhomogeneities alone are unlikely to solve the iron discrepancy.

5.3. *Iron* L *in Other Astrophysical Objects*

Further atomic physics studies may help to assess whether sizable errors were affecting the atomic parameters used in the various thin-plasma emission models. However, a more direct, empirical assessment may come from iron L abundance determinations of astronomical objects whose iron abundance is independently known. In this section we present a preliminary attempt in this direction. It is actually difficult to find individual objects with both well-determined optical and X-ray–determined iron abundances. For most objects in this section, one could argue that the circumstantial evidence may favor near solar abundance. For other objects, e.g., galaxy groups and loose clusters, one may argue that their iron content should not differ greatly from that of rich clusters.

5.3.1. *Binary and Stellar X-Ray Sources*

Strong emission lines are observed during the eclipse of close binary systems. In particular, the eclipse spectrum of Vela X-1 exhibits intense K lines from Fe, Mg, Si, S, and Ar (Nagase et al. 1994). However, as mentioned above, the low fluorescent yield for iron L lines hampers the significant detection of these lines from compact X-ray sources. *ASCA* measurements of stellar X-ray sources β Cet and π^1 UMa (Drake et al. 1994) give the iron abundances $0.77^{+0.24}_{-0.18}$ and $0.41^{+0.24}_{-0.10}$ solar, respectively, while the photospheric iron abundances for these stars obtained by optical measurements are 0.80–0.89 solar (Lambert & Ries 1981; Kovacs 1982) and 0.54 solar (Hearnshaw 1974), respectively. An RS CVn system (AR Lac) suggests that the metallicities including iron L features are a factor of 3–4 below the solar values (White 1996). For AR Lac, Singh, White, & Drake (1996) have derived the iron abundance 0.53 solar with the Meka model by excluding the iron L (0.7–1.74 keV) region. This value is consistent with the optical measurement by Naftilan & Drake (1977), who gave 0.5 solar, but once the iron L region is included the resulting iron abundance becomes as low as 0.29 solar (Singh et al. 1996).

5.3.2. *Supernova Remnants*

Supernova remnants are the rich source of emission lines. In fact, *ASCA* has detected remarkable spectra which are dominated by strong emission lines, e.g., from Cas A (Holt et al. 1994) and W49B (Fujimoto et al. 1995). In connection with the iron L problem in elliptical galaxies, the interesting objects are the SNRs with $kT \simeq 1$ keV. Recent results for three young SNRs (0509−67.5, 0519−69.0, N103B) in the Large Magellanic Cloud with $kT = 1.1$–1.5 keV are reported by Hughes et al. (1995). The observed spectra exhibit strong iron L lines and K lines from Si, S, Ar, and Ca. Lines from O, Ne, and Mg are relatively weak. They show that, qualitatively, the spectra agree well with the W7 model by Nomoto et al. (1984) for SN Ia's. Again, the rough consistency with the model calculation including the iron L lines with the observed data suggests that the model estimation should not differ by more than a factor of 2, at least for $kT \gtrsim 1$ keV. However, the iron abundance in the Cygnus loop, an older and cooler SNR, appears to be appreciably subsolar ($\lesssim 0.1$ solar; Miyata et al. 1994), although its low temperature (~ 0.3 keV) suggests that the objects could be out of ionization equilibrium.

5.3.3. *Starburst Galaxies and AGNs*

ASCA observations of starburst galaxies indicate that the X-ray emission from these systems is not explained by a single component. There seem to be at least three emission components, as best demonstrated for the brightest galaxy, M82 (Tsuru et al. 1994). The observed energy spectrum shows very weak iron K lines, He-like and H-like Si and Mg lines, and the iron L complex. The ratio of H to He-like Si lines indicates a plasma temperature of 1–1.3 keV, which is too high to account for the ratio of H- to He-like Mg lines; this rather suggests a plasma temperature less than ~ 1 keV. This cool component may extend out of the galaxy, judging from the X-ray morphology taken by *ASCA*.

This complex situation makes starburst galaxies rather unsuitable to calibrate the iron L diagnostics. However, a preliminary value of ~ 0.1 solar is suggested for M82 (Tsuru et al. 1994) and NGC 253 (Awaki et al. 1996).

AGNs (in particular Seyfert galaxies) commonly exhibit fluorescent iron K lines. Highly obscured objects emit strong K lines from Fe, Mg, Si, Ar, and S as a result of fluorescence in the surrounding medium irradiated by a strong continuum X-ray source that is centrally located. However, since the fluorescence yield for iron L lines is only about 0.4%, these lines have not been significantly observed from the scattering medium. Iron L lines are seen in the spectrum of Seyfert 2 galaxies in which AGN and starburst activities occur simultaneously (for example, NGC 1068; Ueno et al. 1994). The iron L feature suggests a thermal plasma with $kT \sim 0.6$ keV, and the resulting iron abundance is about 0.3 solar. Therefore, the situation is similar to that of starburst galaxies.

5.3.4. *Groups and Clusters of Galaxies*

The iron L lines have been observed in clusters of galaxies in two broad circumstances: in poor clusters and groups with relatively cool ICM ($kT \lesssim 3$ keV) and in the central

cool regions of large *cooling flow* clusters. The former case includes the NGC 5044 group, HCG 51 (Fukazawa et al. 1996), and the Fornax Cluster (Ikebe 1996). The ICM temperatures are typically $kT \gtrsim 1$ keV, and the iron abundance determined from the iron L lines is 0.3–0.4 solar. These abundances values agree with those determined for rich clusters (with $kT \gtrsim 3$ keV) from the iron K lines, which suggests that the iron abundance may be the same in different classes of clusters (Ohashi 1995). This agreement seems to indicate that the iron L diagnostics are correct, at least at the temperature of these clusters.

However, the situation is different for cooler clusters and groups. For example, an iron abundance as low as 0.06 solar was derived for the NGC 2300 group (Mulchaey et al. 1993; Sakima, Tawara, & Yamashita 1994), whose ICM temperature is 0.9 keV, and a seemingly low abundance has been estimated for the group HCG 62 (cf. Ohashi 1995). The resulting IMLR is exceptionally low for NGC 2300, which has forced RCDP to appeal to a rather contrived scenario, with the group having first suffered extensive gas and iron losses, then followed by reaccretion of matter extensively diluted with pristine material. Figure 5 (adapted from Rezini 1996c), shows the iron abundance of the ICM clusters and groups as a function of their temperature. It is apparent that for $kT \gtrsim 3$ keV the iron abundance (derived for the iron K feature) is fairly constant, a well-known result. However, for lower temperatures iron L features are used, and the ICM iron abundance starts showing large variations that appear systematic with temperature rather than random. For T decreasing from ~ 3 keV to ~ 1 keV the abundance appears to increase, from ~ 0.3 solar to approximately solar. Below ~ 1 keV, however, the abundance drops precipitously to virtually zero (the lowest points in Fig. 5 are actually upper limits at 0.01 solar!), with a tight abundance-temperature correlation. This systematic trend with temperature may find an astrophysical explanation, but it would indeed be more naturally understood as the result of a systematic bias of the iron L diagnostics, with iron being overestimated for $kT \sim 1$ keV (when Fe XXIV–Fe XXV dominate), and progressively more and more underestimated at lower temperatures, when lower and lower ionization stages (down to Fe XVI) become responsible for the iron L emission. Actually, this trend may provide some hint

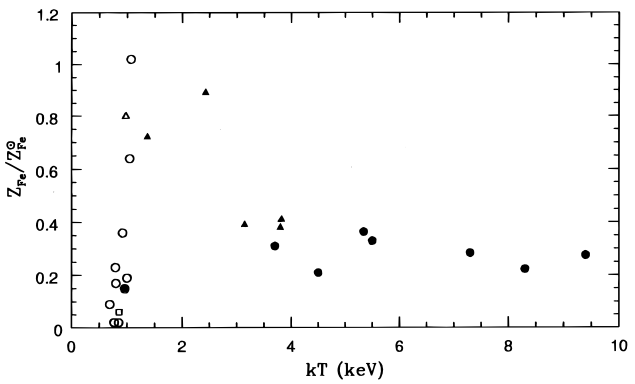

FIG. 5.—Iron abundance of the ICM of clusters and groups as a function of the ICM temperature. Data are taken from the following sources: *Filled circles*: Arnaud et al. (1992); *filled triangles*: Tsuru (1993); *open triangles*: David et al. (1994); *open squares*: Mulchaey et al. (1993); *filled squares*: Ponman et al. (1994); *open circles*: Mulchaey et al. (1996). For $kT \gtrsim 3$ keV the iron abundance derived from the iron K complex, while for lower temperatures the iron L complex is used.

as to which aspect of the atomic physics may be called into question.

An interesting case of a rich cluster with a cool core is the Centaurus Cluster (Fukazawa et al. 1994; Ikebe 1996). The temperature of the widely spread ICM is 3.8 keV, but the energy spectrum in the central ~ 300 kpc region shows clear presence of cooler, ~ 1 keV gas characterized by strong iron L lines. The spectral fit indicates that the metal abundances of both hot and cool gas are consistent with being the same, both rising to about 1.7 solar in the center from 0.3 solar in the cluster outskirts. However, the two-component (or multicomponent) nature of the spectrum makes the independent abundance determination using only iron L lines difficult. In fact, if one lets kT and the abundance of the cool component vary freely, they remain undetermined. Nonetheless, the consistency of the abundance with the hot component suggests that the iron L line diagnostics may not be affected by large systematic errors, at least at the temperature of such a cool component (kT slightly above 1 keV).

6. DISCUSSION AND CONCLUSIONS

The iron abundance in the ISMs of elliptical galaxies—as derived from X-ray observations of the iron L complex—appears to be as low as 0.1–0.4 solar. Such low abundances are at variance with the abundance expected from the stellar population as derived from current population synthesis methods of the optical spectrum, especially if allowance is made for further enrichment by SN Ia's at empirically determined rates, which together imply an abundance $\gtrsim 2$ times solar. This strong discrepancy appears to shake our understanding of supernova enrichment and chemical evolution of galaxies.

If the ISM iron abundances indicated by X-ray observations are correct, then not only should population synthesis methods be in error, but also either the empirical SN Ia rate in ellipticals or the current theoretical estimates of the iron yield of these SNs should be in error. Moreover, the iron share between the ICM and cluster galaxies would change from being nearly equal, to most of iron being in the ICM, with the ICM containing $\sim \frac{5}{6}$ of the total iron, and stars in galaxies only $\sim \frac{1}{6}$. This would imply a dramatic mass loss from galaxies at early times, and along with it a very strong heating of the ICM that would have major effects on the evolution of the ICM itself.

Formally, the X-ray observations seem to require the SN Ia activity to be virtually suppressed in cluster ellipticals, compared to spiral galaxies. However, we point out that binary star indicators such as the nova rate and the ratio of hard X-ray to optical luminosity in ellipticals suggest that the binary star population is virtually the same as in spiral galaxies. Other astrophysical explanation of the discrepancy, such as hiding iron in solid particles or in Jupiter-like objects, or diluting it with an iron-poor ICM, do not appear to be promising.

Having failed to find an attractive astrophysical solution, we have explored the opposite option, scrutinizing in some detail the tool used in deriving iron abundances from X-ray spectra. It is found that three different thin-plasma models give basically the same iron abundances when applied to astrophysical thin plasmas with $kT \gtrsim 3$ keV. However, for lower temperatures, and especially for $kT \lesssim 1$ keV, different codes can give iron abundances that differ by as much as a factor of 3. The complex nature of the iron ions responsible

for the iron L emission around 1 keV is probably to blame for these discrepancies, since the atomic physics parameters of these ions are poorly known. This suspicion is somewhat reinforced by several empirical results, indicating iron abundances systematically below solar when temperatures lower than ~ 1 keV are encountered. This is the case of objects as disparate as binary X-ray stars such as RS CVn's and Algols, SN remnants, starburst galaxies, and galaxy groups. The latter is an especially clear case: the intragroup iron abundance seems to drop by 2 orders of magnitude for $kT \lesssim 1$ keV.

All this evidence, coupled to the failure of our attempts to find a reasonable astrophysical explanation, suggest to us that it is worthwhile to explore further the possiblity that the very low iron content derived from X-ray observations may be an artifact of the thin-plasma model tools employed in the diagnostics of the iron L X-ray emission complex. While we believe it is worthwhile to continue to reconsider critically our views of the enrichment process of galaxies, groups, and clusters, we also believe it is worthwhile to extend such a critical attitude to X-ray diagnostic tools.

We are grateful to our referee, Michael Loewenstein, for his useful and detailed constructive suggestions. This work was financially supported in part by Grants-in-Aid for Scientific Research (N. A.; Nos. 06640349 and 07222206) by the Japanese Ministry of Education, Culture, Sport, and Science. A. R. gratefully acknowledges the support of the Japan Society for the Promotion of Science (JSPS), which made possible an extended visit to the University of Tokyo during which this project was started. K. M. and Y. I. acknowledge financial supprt from the JSPS.

REFERENCES

Abia, C., Canal, R., & Isern, J. 1991, ApJ, 366, 198
Arimoto, N., & Yoshii, Y. 1987, A&A, 173, 23
Arnaud, M., Rothenflug, R., Boulade, O., Vigroux, R., & Vangioni-Flam, E. 1992, A&A, 254, 49
Arnette, W. D., Branch, D., & Wheeler, J. C. 1985, ApJ, 295, 589
Awaki, H., et al. 1994, PASJ, 46, L65
———. 1996, in UV and X-Ray Spectroscopy of Astrophysical and Laboratory Plasmas, ed. Y. Yamashita & T Watanabe (Tokyo: Universal Academy Press), 327
Awaki, H., Koyama, K., Kunieda, H., Takano, S., Tawara, Y., & Ohashi, T. 1991, ApJ, 366, 88
Barbuy, B. 1992, in The Stellar Populations of Galaxies, ed. B. Barbuy & A. Renzini (Dordrecht: Kluwer), 143
Baum, W. A., Thomsen, B., & Morgan, B. L. 1986, ApJ, 301, 83
Bessell, M. S., Sutherland, R. S., & Ruan, K. 1991, ApJ, 383, L71
Bica, E. 1988, A&A, 195, 75
Binney, J., & Tabor, G. 1995, MNRAS, 276, 663
Boroson, T. A., & Thompson, I. B. 1991, AJ, 101, 111
Branch, D., Livio, M., Yungelson, L. R., Boffi, F. R., & Baron, E. 1995, PASP, 107, 1019
Buzzoni, A., Gariboldi, G., & Mantegazza, L. 1992, AJ, 103, 1814
Canizares, C. R., Fabbiano, G., & Trinchieri, G. 1987, ApJ, 312, 503
Cappellaro, E., Turatto, M., Benetti, S., Tsvetkov, D. Yu., Bartunov, O. S., & Makarova, I. N. 1993, A&A, 268, 472
Carlberg, R. 1985, ApJ, 286, 404
Carollo, C. M., & Danziger, I. J. 1994a MNRAS, 270, 523
———. 1994b, MNRAS, 270, 743
Cavaliere, A., Colafrancesco, S., & Menci, N. 1993, ApJ, 415, 50
Ciotti, L., D'Ercole, A., Pellegrini, S., & Renzini, A. 1991, ApJ, 376, 380
Ciotti, L., & Ostriker, J. 1996, in preparation
Clegg, R. E. S. 1989, in Planetary Nebulae, ed. S. Torres-Peimbert (Dordrecht: Kluwer), 139
Couture, J., & Hardy, E. 1988, AJ, 96, 867
David, L. P., Forman, W., & Jones, C. 1990, ApJ, 359, 29
David, L. P., Jones, C., Forman, W., & Daines, S. 1994, ApJ, 428, 544
Davidge, T. J. 1992, AJ, 103, 1512
Davies, R. L., Burstein, D., Dressler, A., Faber, S. M., Lynden-Bell, D., Terlevich, R. J., & Wegner, G. 1987, ApJS, 64, 581
Davies, R. L., Sadler, E. M., & Peletier, R. F. 1993, MNRAS, 262, 650
Delisle, S., & Hardy, E. 1992, AJ, 103, 711
Della Valle, M., Rosino, L., Bianchini, A., & Livio, M. 1994, A&A, 287, 403
de Vaucouleurs, G. 1948, Ann. d'Astrphys., 11, 247
Donnelly, R. H., Faber, S. M., & O'Connell, R. M. 1990, ApJ, 354, 52
Dow, K. L., & White, S. D. M. 1995, ApJ, 439, 113
Drake, S. A., Singh, K. P., White, N. E., & Simon, T. 1994, ApJ, 436, L87
Efstathiou, G., & Gorgas, J. 1985, MNRAS, 215, 37P
Elbaz, D., Arnaud, M., & Vangioni-Flam, E. 1995, A&A, 303, 345
Fabbiano, G. 1995, in ASP Conf. Ser. 86, Fresh Views of Elliptical Galaxies, ed. A. Buzzoni, A. Renzini, & A. Serrano (San Francisco: ASP), 103
Fabbiano, G., Kim, D.-W., & Trinchieri, G. 1992, ApJS, 80, 531
———. 1994, ApJ, 429, 94
Faber, S. M. 1977, in The Evolution of Galaxies and Stellar Populations, ed. B. M. Tinsley & R. B. Larson (New Haven: Yale Univ. Obs.), 157
Fabian, A. C., Arnaud, K. A., Bautz, M. W., & Tawara, Y. 1994, ApJ, 436, L63
Fabian, A. C., Thomas, P. A., Fall, S. M., & White, R. E., III. 1986, MNRAS, 221, 1049
Forman, W., Jones, C., David, L., Franx, M., Makishima, K., & Ohashi, T. 1993, ApJ, 418, L55
Franx, M., Illingworth, G., & Heckman, T. 1989, AJ, 98, 538
Freedman, W. 1989, AJ, 98, 1285
Fujimoto, R., et al. 1995, PASJ, 47, L31
Fukazawa, Y., et al. 1994, PASJ, 46, L141
———. 1996, PASJ, in press
Gorgas, J., Efstathiou, G., & Aragón-Salamanca, A. 1990, MNRAS, 245, 217
Gratton, R., & Ortolani, S. 1986, A&A, 169, 201
Greggio, L. 1996, in The Interplay between Massive Star Formation, the ISM, and Galaxy Evolution, ed. D. Kunth, B. Guiderdoni, M. Heydari-Malayeri, T. X. Thuan, & J. T. Thanh Van (Gif-sur-Yvette: Editions Frontières), in press
———. 1997, MNRAS, in press
Greggio, L., & Renzini, A. 1983a, A&A, 118, 217
———. 1983b, Mem. Soc. Astron. Italiana, 54, 311
Hearnshaw, J. B. 1974, A&A, 34, 263
Holt, S. S., Gotthelt, E. W., Tsunemi, H., & Negoro, H. 1994, PASJ, 46, L151
Hughes, J. P., et al. 1995, ApJ, 444, L81
Iben, I., Jr., & Tutukov, A. V. 1984, ApJS, 54, 335
Ikebe, Y. 1996, Ph.D. thesis, Univ. Tokyo, RIKEN, IPCR CR-87
Ikebe, Y., et al. 1992, ApJ, 384, L5
Ishimaru, Y., & Arimoto, N. 1997, PASJ, in press
Itoh, H. 1989, PASJ, 41, 853
Kaastra, J. S. 1992, An X-Ray Spectral Code for Optically Thin Plasmas (Internal SRON-Leiden Rep., updated version 2.0)
Kaiser, N. 1991, ApJ, 383, 104
Kim, D.-W., Fabbiano, G., & Trinchieri, G. 1992, ApJ, 393, 134
Kodaira, K., Okamura, S., Ichikawa, S., Hamabe, M., & Watanaba, M. 1990, Photometric Catalog of Northern Bright Galaxies, Institute of Astronomy, Univ. Tokyo
Kovacs, N. 1982, A&A, 120, 21
Kritsuk, A. G. 1992, A&A, 261, 78
Lambert, D. L., & Ries, L. M. 1981, ApJ, 248, 228
Larson, R. B. 1974, MNRAS, 169, 229
———. 1976, MNRAS, 176, 31
Liedahl, D. A., Osterheld, A. L., & Goldstein, W. H. 1995, ApJ, 438, L115
Loewenstein, M., & Mathews, W. G. 1991, ApJ, 373, 445
Loewenstein, M., & Mushotzky, R. F. 1996, ApJ, 471, L83
Loewenstein, M., Mushotzky, R. F., Tamura, T., Ikebe, Y., Makishima, K., Matsushita, K., Awaki, H., & Serlemitsos, P. J. 1994, ApJ, 436, L75
Makishima K., et al. 1996, PASJ, 48, 171
Masai, K. 1984, Ap&SS, 98, 367
Mathews, W. G. 1990, ApJ, 354, 468
Matsushita, K., et al. 1994, ApJ, 436, L41
Matteucci, F., & François, P. 1992, A&A, 262, L1
Matteucci, F., & Gibson, B. K. 1995, preprint
Matteucci, F., & Greggio, L. 1986, A&A, 154, 279
Metzler, C. A., & Evrard, A. E. 1994, ApJ, 437, 564
Mewe, R., Gronenschild, E. H. B. M., & van den Oord, G. H. J. 1985, A&AS, 62, 197
Mewe, R., Lemen, J. R., & van den Oord, G. H. J. 1986, A&AS, 65, 511
Miyata, E., Tsunemi, H., Pisarski, R., & Kissel, S. E. 1994, PASJ, 46, L101
Mould, J. R. 1978, ApJ, 220, 434
Mulchaey, J. S., Davis, D. S., Mushotzky, R. F., & Burstein, D. 1993, ApJ, 404, L9
———. 1996, ApJ, 456, 80
Murray, S. D., & Balbus, S. A. 1992, ApJ, 395, 99
Mushotzky, R. 1994, in Clusters of Galaxies, ed. F. Durret (Gif-sur-Yvette: Editions Frontières), 167
Mushotzky, R. F., Loewenstein, M., Awaki, H., Makishima, K., Matsushita, K., & Matsumoto, H. 1994, ApJ, 436, L79
Mushotzky, R. F., et al. 1996, ApJ, 466, 686
Naftilan, S. A., & Drake, S. A. 1977, ApJ, 216, 508
Nagase, F., et al. 1994, ApJ, 436, L1
Nomoto, K., Thielemann, F.-K., & Yokoi, K. 1984, ApJ, 286, 644

Nomoto, K., et al. 1993, in Elements and the Cosmos, ed. R. J. Terlevich, B. E. J. Pagel, R. Carswell, & M. Edmunds (Cambridge: Cambridge Univ. Press), 55
Nomoto, K., Yamaoka, H., Shigeyama, T., & Iwamoto, K. 1996, in Supernovae and Supernova Remnants, ed. R. McCray & Z. Wang (Cambridge: Cambridge Univ. Press), 49
O'Connell, R. W. 1986, in Spectral Evolution of Galaxies, ed. C. Chiosi & A. Renzini (Dordrecht: Reidel), 321
Ohashi, T. 1995, Ann. NY Acad. Sci., 759, 217
Ohashi, T., et al. 1996, PASJ, 48, 157
Ohashi, T., & Tsuru, T. 1992, in Frontiers of X-Ray Astronomy, ed. Y. Tanaka, & K. Koyama (Tokyo: Universal Academy Press), 435
Ohashi, T., et al. 1990, in Windows on Galaxies, ed. G. Fabbiano, J. Gallagher, & A Renzini (Dordrecht: Kluwer), 243
Peletier, R. F., Davies, R. L., Illingworth, G. D., Davis, L., & Cawson, M. 1990, AJ, 100, 1091
Pellegrini, S. 1994, A&A, 292, 395
Pellegrini, S., & Fabbiano, G. 1994, ApJ, 429, 105
Ponman, T. J., et al. 1994, Nature, 369, 462
Raymond, J. C., & Smith B. W. 1977, ApJS, 35, 419
Renzini, A. 1994a, in Panchromatic View of Galaxies, ed. G. Hensler et al. (Gif-sur-Yvette: Editions Frontières), 155
———. 1994b, in Clusters of Galaxies, ed. F. Durret et al. (Gif-sur-Yvette: Editions Frontières), 221
———. 1996a, in Supernovae and Supernova Remnants, ed. R. McCray & Z. Wang (Cambridge: Cambridge Univ. Press), 77
———. 1996b, in New Light on Galaxy Evolution, ed. R. Bender & R. Davies (Dordrecht: Kluwer), 131
———. 1996c, in preparation
Renzini, A., Ciotti, L., D'Ercole, A., & Pellegrini, S. 1993, ApJ, 419, 52 (RCDP)
Ruiz-Lapuente, P., Burkert, A., & Canal, R. 1996, ApJ, 447, L69
Sakima, Y., Tawara, Y., & Yamashita, K. 1994, in New Horizon of X-Ray Astronomy: First Results from *ASCA* (Tokyo: Universal Academy Press), 557
Sarazin, C. L. 1986, Rev. Mod. Phys., 58, 1
Serlemitos, P. J., Loewenstein, M., Mushotzky, R. F., Marshall, F. E., & Petre, R. 1993, ApJ, 413, 518
Shigeyama, Y., Nomoto, K., Yamaoka, H., & Thielemann, F.-K. 1992, ApJ, 386, L13
Singh, K. P., White, N. E., & Drake, S. A. 1996, ApJ, 456, 766
Sneden, C., Lambert, D. L., & Whitaker, R. W. 1979, ApJ, 234, 964
Takano, S. 1989, Ph.D. thesis, Univ. Tokyo
Tammann, G. 1982, in Supernovae: A Survey of Current Research, ed. M. Rees & R. Stoneham (Dordrecht: Reidel), 371
Tanaka, Y., Inoue, H., & Holt, S. S. 1994, PASJ, 46, L37
Thomsen, B., & Baum, W. A. 1987, ApJ, 315, 460
Timmes, F. X., Woosley, S. E., & Weaver, T. A. 1995, ApJS, 98, 617
Tinsley, B. M. 1980, Fundam. Cosmic Phys., 5, 287
Trinchieri, G., Kimm, D.-W., Fabbiano, G., & Canizares, C. R. 1994, ApJ, 428, 555
Tsuru, T. 1993, Ph.D. thesis, Univ. Tokyo, ISAS RN 528
Tsuru, T., et al. 1994, in New Horizon of X-Ray Astronomy, ed. F. Makino & T. Ohashi (Tokyo: Universal Academy Press), 529
Tully, R. B. 1988, Nearby Galaxies Catalog (Cambridge: Cambridge Univ. Press)
Ueno, S., et al. 1994, PASJ, 46, L71
van den Bergh, S., & Tammann, G. 1991, ARA&A, 29, 363
Wheeler, J. C., Sneden, C., & Truran, J. W. 1989, ARA&A, 27, 279
White, N. E. 1996, in ASP Conf. Ser., Cool Stars, Stellar Systems, and the Sun, ed. N. Pallavicini & A. K. Dupree (San Francisco: ASP), in press
White R. E., III, & Sarazin, C. L. 1991, ApJ, 367, 476
White, S. D. M., Navarro, J. F., Evrard, A. E., & Frenk, C. S. 1993, Nature, 366, 429
Woosley, S. E., & Weaver, T. A. 1994, in Les Houches, Session LIV, Supernovae, ed. S. R. Bludman, R. Mochkovitch, & J. Zinn-Justin (Kidlington: Elsevier), 63
Worthey, G. 1994, ApJS, 95, 107
Worthey, G., Faber, S. M., & González, J. J. 1992, ApJ, 398, 69